JOURNAL OF GEOPHYSICAL RESEARCH, VOL. 108, NO. B6, 2319, doi:10.1029/2001JB000644, 2003

New insights on the tectonics along the New Hebrides subduction zone based on GPS results

Stéphane Calmant,[1] Bernard Pelletier, and Pierre Lebellegard
Laboratoire de Géophysique, Centre IRD, Noumea, New Caledonia, France

Michael Bevis
Hawaii Institute for Geophysics and Planetology, School of Ocean and Earth Science and Technology, University of Hawaii, Honolulu, Hawaii, USA

Frederick W. Taylor
Institute for Geophysics, University of Texas at Austin, Austin, Texas, USA

David A. Phillips
Hawaii Institute for Geophysics and Planetology, School of Ocean and Earth Science and Technology, University of Hawaii, Honolulu, Hawaii, USA

Received 25 May 2001; revised 7 November 2002; accepted 28 February 2003; published 27 June 2003.

[1] At the New Hebrides (NH) subduction zone, ridges born by the subducting Australia plate enter the trench and collide with the overriding margin. Results from GPS surveys conducted on both sides of the trench and new bathymetry maps of the NH archipelago bring new light on the complex tectonics of this area. Convergence vectors present large variations that are not explained by Australia/Pacific (A/P) poles and that define four segments. Vectors remain mostly perpendicular to the trench and parallel to the earthquake slip vectors. Slow convergence (i.e., 30–40 mm/yr) is found at the central segment facing the D'Entrecasteaux Ridge. The southern segment moves faster than A/P motion predicts (89 to 124 mm/yr). Relatively to a western North Fiji basin (WNFB) reference, the northern and southern segments rotate in opposite directions, consistently with the extension observed in the troughs east of both segments. Both rotations combine in Central Vanuatu into an eastward translation that ''bulldozes'' the central segment into the WNFB at ~55 mm/yr. That model suggests that the motion of the central segment, forced by the subduction/collision of the D'Entrecasteaux ridge, influences the motion of the adjoining segments. The New Caledonia archipelago is motionless with respect to the rest of the Australia plate despite the incipient interaction between the Loyalty ridge and the NH margin. Southeast of the interaction area, convergence is partitioned into a ~50 mm/yr trench-normal component accommodated at the trench and a ~90 mm/yr trench-parallel component, close to the A/P convergence, and presumably accommodated by a transform boundary at the rear of the NH arc. *INDEX TERMS:* 1206 Geodesy and Gravity: Crustal movements—interplate (8155); 1243 Geodesy and Gravity: Space geodetic surveys; 3040 Marine Geology and Geophysics: Plate tectonics (8150, 8155, 8157, 8158); 8158 Tectonophysics: Plate motions—present and recent (3040); 9355 Information Related to Geographic Region: Pacific Ocean; *KEYWORDS:* plate tectonics using GPS, convergent margin, New Hebrides subduction zone, New Caledonia, North Fiji Basin, southwest Pacific

Citation: Calmant, S., B. Pelletier, P. Lebellegard, M. Bevis, F. W. Taylor, and D. A. Phillips, New insights on the tectonics along the New Hebrides subduction zone based on GPS results, *J. Geophys. Res.*, *108*(B6), 2319, doi:10.1029/2001JB000644, 2003.

1. Introduction

[2] The convergence boundary between the Australian and Pacific plates corresponds to a broad area of deformation characterized by the opposite-facing and partly overlapping Tonga and New Hebrides (NH) subduction zones, behind and between which back arc extension occurs in the Lau and North Fiji Basins (NFB) (Figure 1). The NH trench marks the eastward subduction of the Australian plate beneath the NH arc and the NFB, a back arc basin resulting from complex spreading [*Auzende et al.*, 1995]. The overriding plate is bordered along this trench by the NH arc. This arc is composed primarily of both active and quiescent volcanoes. The central arc, however, is composed

[1]Now at Laboratoire de Géophysique et Océanographie Spatiale, Toulouse, France.

0148-0227/03/2001JB000644$09.00

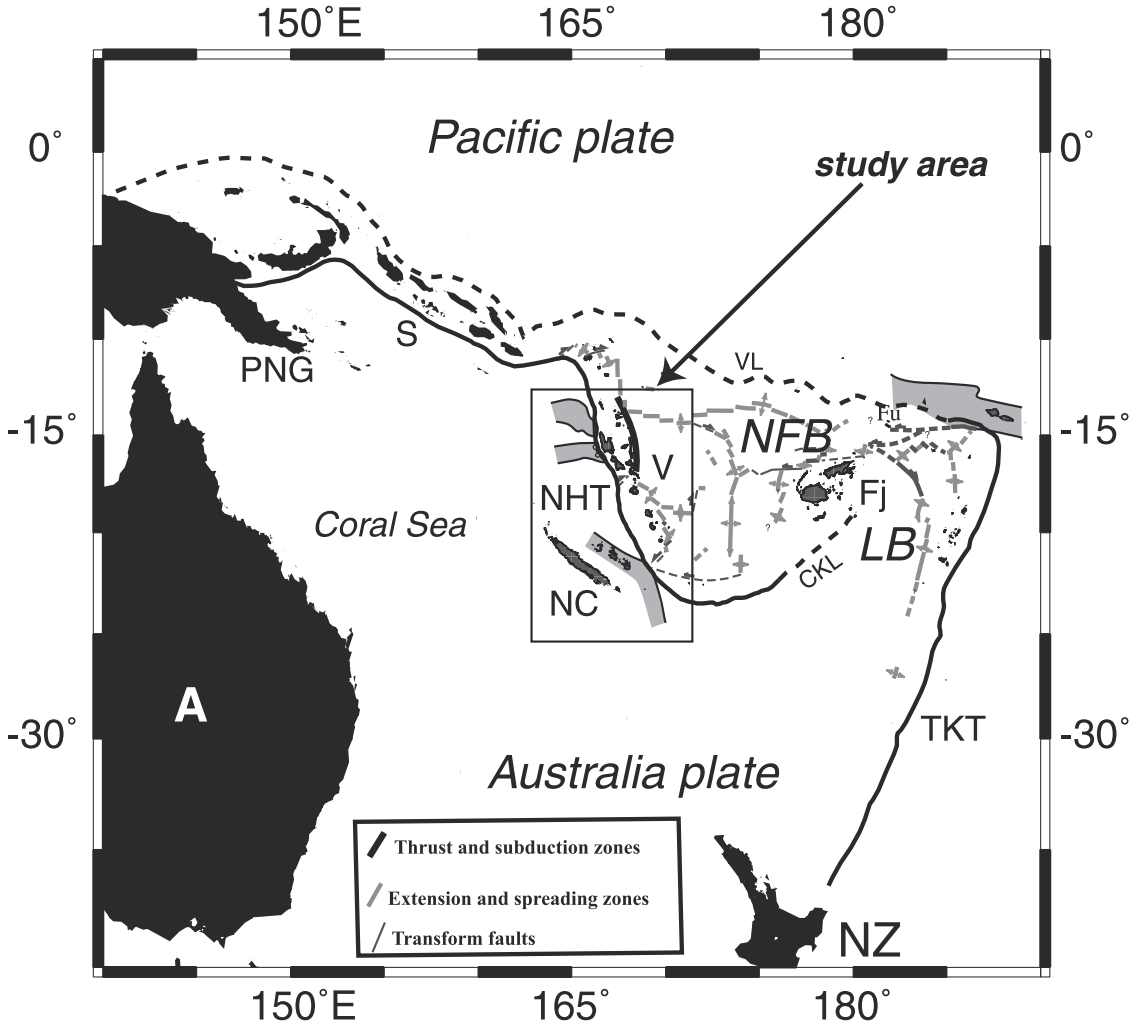

Figure 1. Situation map of the study area in southwest Pacific. Thick lines represent the following major plate boundaries: Tonga (TT), Kermadec (KT), and New Hebrides (NHT) trenches. Dashed line represents the Vitiaz Trench Lineament (VL), remnant of the former Australia-Pacific convergence boundary and the Conway-Kandavu Lineament (CKL). NFB, North Fiji Basin; LB, Lau Basin; A, Australia; PNG, Papua New Guinea; NC, New Caledonia; V, Vanuatu; S, Solomon Islands; Fj, Fiji; NZ, New Zealand; and Fu, Futuna-Nui.

of older island arc series which have been uplifted due to interaction with the D'Entrecasteaux ridge (DER), an aseismic feature born by the downgoing Australian plate [*Collot et al.*, 1985]. Facing the southern part of the NH arc, the Australian plate bears the NW-SE trending Loyalty ridge (LR) that interacts with the NH trench (incipient collision) near 22°S [*Maillet et al.*, 1989; *Monzier et al.*, 1990]. This area faces then two distinct types of subduction of lithospheric asperity. First is a collision of two narrow seamount chains, the DER, that started 2 Ma ago at Central Vanuatu. Second is an incipient interaction with a broad ridge of continental core, the LR, at the southern virgation of the trench.

[3] In the present study, we interpret Global Positioning System (GPS) times series collected on islands across the trench together with updated bathymetry maps. These data are used to infer the consequences of these asperity subductions on the tectonics of the subducting plate itself and on the tectonics of the margin that overrides the subducting plate, namely the NH arc, including its interactions with the NFB at its back.

2. GPS Data

2.1. Field Operations

[4] The first data that we used were collected in 1990 and 1992 as part of the southwest Pacific GPS Project (SWP) [*Schutz et al.*, 1993; *Bevis et al.*, 1995; *Taylor et al.*, 1995] using Trimble SSE dual frequency GPS receivers. From 1992 to 1996, we continued to survey a few sites within the Vanuatu and New Caledonia (NC) archipelago using Leica SR299 dual-frequency receivers. In 1996, we equipped four continuous GPS (CGPS) sites with Ashtech Z-12 dual-frequency receivers and choke ring antennas. Two sites were established on the Australian plate to serve as stable reference sites (Figure 2): one (KOUC) northwest of Grande Terre, NC, and the other (LPIL) on Lifou, within the Loyalty archipelago. The other two CGPS sites were

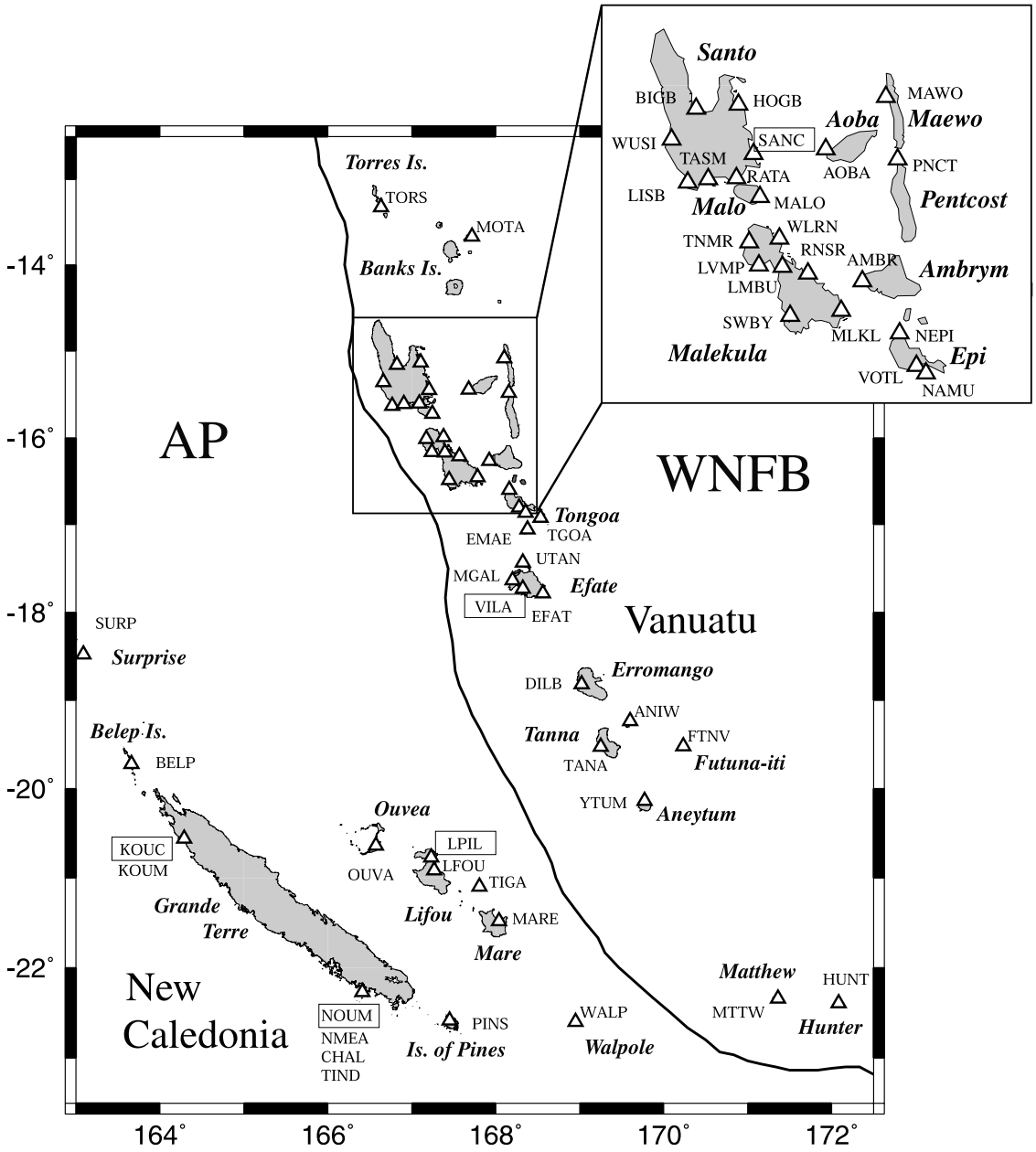

Figure 2. Location of Global Positioning System sites with four character identifiers. Dense network in Central Vanuatu is enlarged in upper right corner. CGPS site names are surrounded by boxes. Labels: AP, Australian plate; and WNFB, western North Fiji Basin.

installed in Vanuatu, on Santo (SANC) and Efate (VILA). In November 1997, the Survey Department of New Caledonia installed a CGPS site in Noumea, NC (NOUM), equipped with a Trimble 4000 SSI dual-frequency receiver and choke ring antenna. This site is now included in the International Terrestrial Reference Frame (ITRF) as an International GPS Geodynamics Service (IGS) site. Last, a CGPS was set in mid-1998 at Futuna Island, northeast of Fiji (Figure 1). The network was extended from 1996 to encompass the whole country of Vanuatu, from the Torres Islands in the north to Aneytum in the south, and densified in Central Vanuatu (Figure 2).

[5] The GPS surveys conducted in the southernmost part of the NH subduction zone deserve special mention. Because of logistic constraints, the surveys conducted on these islets were short with respect to the baseline lengths: 24–36 hours at Walpole, 12–24 hours at Matthew, and only 2–12 hours at Hunter. Moreover, these sites were all surveyed using LEICA SR299 or SR399 dual-frequency receivers, systems lacking accurate antenna models. Results obtained from these receivers were therefore noticeably worse than those obtained from the Ashtech Z-12 receivers and choke ring antennas, especially in the vertical component where scatter of several centimeters is suffered. As far as the sites at Matthew and Hunter are concerned, it can be mentioned that some local, short-period motion due to volcanic activity cannot be fully discarded, although no unusual activity was noticed during the observation period.

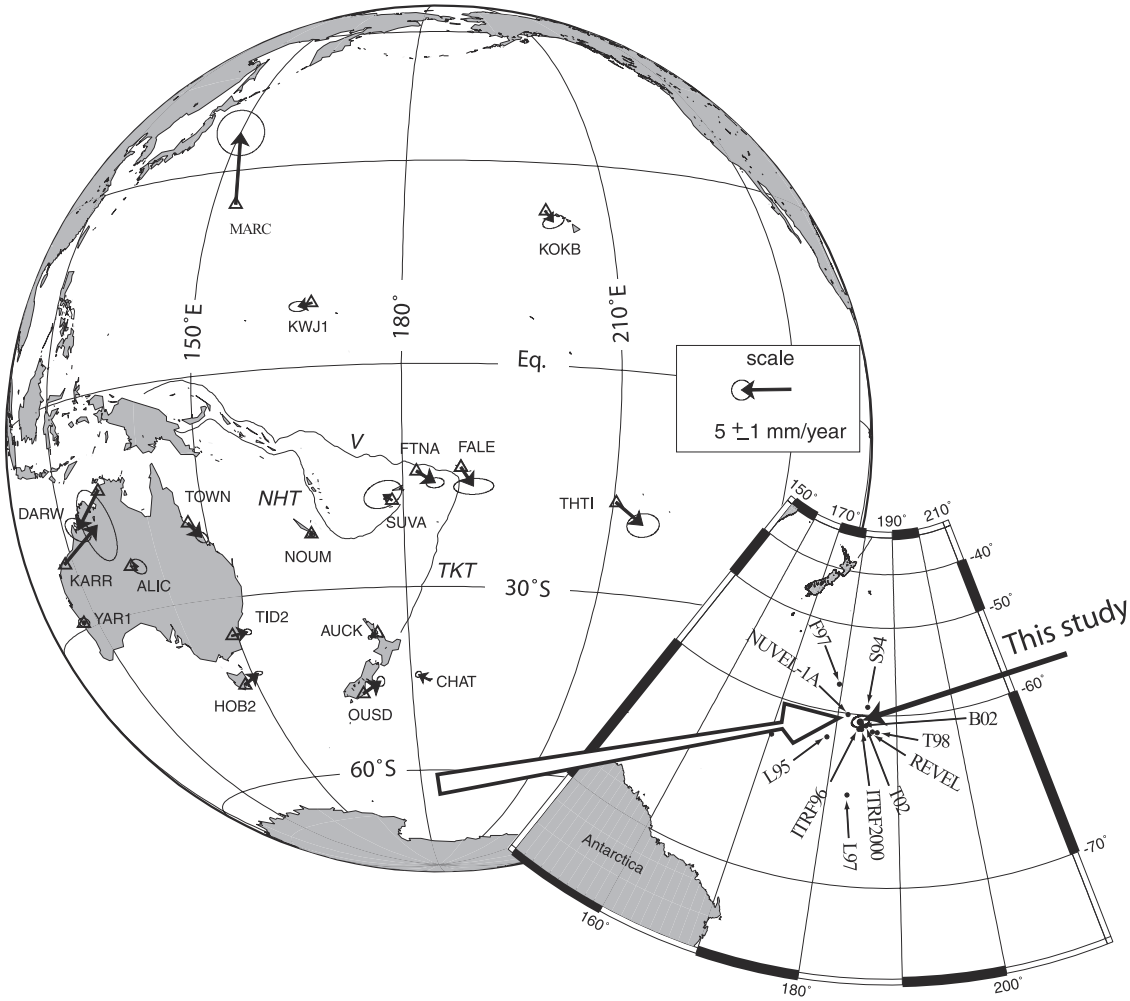

Figure 3. CGPS sites used to constrain the local network solutions. Arrows show residual velocities relative to the best fitting poles for the Australian and Pacific plates. Labels of tectonic boundaries: V, Vitiaz Trench Lineament; TKT, Tonga-Kermadec Trench; NHT, New Hebrides Trench. Lower right inset: close-up view of the location of poles for selected Euler vectors for A/P motion. These Euler vectors were determined by different techniques that encompass different timescales: GPS only for L95 [*Larson and Freymueller*, 1995], L97 [*Larson et al.*, 1997], T98 [*Tregoning et al.*, 1998], T02 [*Tregoning*, 2002]; REVEL [*Sella et al.*, 2002]; B02 [*Beavan et al.*, 2002]; SLR only for S94 [*Smith et al.*, 1994]; combination of space geodesy techniques for ITRF96 and ITRF 2000; worldwide combination of seismic vectors and marine geophysical data for NUVEL-1A [*De Mets et al.*, 1994], and local seismicity for F97 [*Frohlish et al.*, 1997]. ITRF 96 was computed from Euler vectors of absolute motion published by *Sillard et al.* [1998]. ITRF 2000 solution was computed from the table of velocities published by IGN (www.ign.fr).

[6] Except for the above mentioned southernmost sites, all observations consisted of at least three 24-hour sessions. GPS data were recorded at 30-s intervals. Whenever possible, we used masts instead of tripods to support the GPS antenna. Masts greatly reduced potential antenna setup errors because there is no centering error if properly leveled, and no antenna height measurement is needed. About 90% of the sites were surveyed using these masts from mid-1996 onward. Tripods were used at all sites from 1990 to early 1996 and at the remaining 10% after mid-1996, mostly on Malekula Island.

2.2. Data Processing

[7] For the purpose of computations, we included in our data set additional CGPS sites located on the Australian and Pacific plates (Figure 3). Some of these sites are IGS sites and/or ITRF sites. Others are maintained by independent research agencies. The goal of including such sites in our computations is twofold. In terms of geodesy, the goal is to be able to constrain our daily solutions of site positions with respect to the ITRF 2000 reference frame. In terms of plate tectonics, the goal is to be able to compute rotation poles for the Australian and Pacific plates and express station velocity solutions with respect to fixed Australian or Pacific plates. The data time series spans from 1990 to early 2001. From 1990 until mid-1996, solutions were computed only for the days when the local network was surveyed. After mid-1996, when our CGPS network was established daily solutions were computed. The GPS observations were processed using "Bernese"

Table 1. Euler Poles Best Fitting the Continuous Global Positioning System Site Motions on the Australian and Pacific Plates[a]

	Ω, deg/Ma	Latitude of Pole	Longitude of Pole
Ω_A	0.6077 ± 0.0031	31.54 ± 0.12°N	37.84 ± 0.39°E
Ω_P	0.6765 ± 0.0067	63.40 ± 0.34°S	111.15 ± 1.33°E
$\Omega_{A/P}$	1.061 ± 0.009	60.62 ± 0.45°S	183.89 ± 0.31°E

[a]Reported uncertainties are 1σ scaled by the unit covariance factor (1.4). Ω_A, Australian plate; Ω_P, Pacific plate; and $\Omega_{A/P}$, Australian/Pacific relative motion.

software [*Rotacher et al.*, 1993]. IGS precise orbit, pole, and clock files were used. Antenna models were obtained from the University of Bern and the Bernese software. Processing was performed in several steps. First, all the daily solutions (about 1500) were computed in the same reference frame as the orbits. Second, all these solutions were converted to ITRF 2000 solutions by applying available Helmert transformations. However, these global transformations do not provide as good an adjustment to the velocity field as our subset of ITRF sites. Accordingly, our regional subset of CGPS stations was not motionless with respect to the ITRF 2000 Euler poles for the Australian and Pacific plates. We therefore computed the Euler poles that best fit the velocity field of our regional CGPS stations. These best fitting Euler poles are reported in Table 1. The Euler pole of greatest interest to this study is the pole of relative motion between the Australian and Pacific plates. Our solution, $\Omega_{A/P}$, is reported in Table 1 and is compared geographically to other pole solutions in Figure 3. As expected, our solution lies close to the ITRF 2000 solution since it is but a second-order correction from the latter. It also lies well inside the area encompassed by all the other solutions, bringing confidence to the validity of our solution. Australia/Pacific (A/P) relative motion derived from the pole $\Omega_{A/P}$ will be used for the remainder of this discussion and will be referred to as simply A/P.

[8] Residuals between observed and pole-predicted velocities are reported in Table 2 and Figure 3 for all the regional CGPS stations used to compute the best fitting Euler poles. The RMS discrepancy between observed and predicted velocities are 2.8 and 1.3 mm/yr for the Pacific and Australian plates, respectively. For sites described in ITRF 2000 and included in our study, Table 2 also reports the residual motions (1) between observed velocities, velocities predicted by our calculated A/P pole, and velocities predicted by ITRF 2000, and (2) between velocities published by ITRF 2000 and those predicted by the ITRF 2000 pole. In particular, RMS discrepancies between ITRF 2000 reported and predicted velocities are 1.7 and 2 mm/yr for the Pacific and Australian plates, respectively. Thus discrepancies between observed and pole-derived velocities in our study compare well to those in ITRF 2000.

[9] In all the inversion schemes, e.g., determination of Helmert parameters and fit of the time series, observations were weighted according to the formal covariance matrices issued by Bernese. As far as the fit of the time series is concerned, observations were grouped by campaigns so that unit covariance factors between the daily observations of a campaign and their average could be calculated and used to scale the uncertainty associated with each average position. Ten-day sessions were considered for CGPS data. Then, the unit covariance factor between the series of average positions and the model of reference position and rate was used to scale the uncertainties associated with these reference positions and velocities. Therefore the uncertainties reported for the velocity estimates actually account for the scatter between the daily observations and the adjusted model of motion without inverting the large matrix systems that hundreds of daily observations would imply. Typical RMS between session-average and linear-fit positions is less than

Table 2. Residual Motion of Continuous Global Positioning Systems Sites on the Australian and Pacific Plates Relative To Rigid Plate Poles

Site		Velocity Residuals: GPS Versus Ω_P Model and ITRF 2000 (in Parentheses), mm/yr		Velocity Residuals: ITRF 2000 Published Versus ITRF 2000 Pole Predicted, mm/yr	
Name	Location	E-W	N-S		
		Australian Plate			
ALIC	133.89°E, 23.67°S	0.8 ± 0.7(1.0)	−0.2 ± 0.8(1.0)	0.2 ± 3.0	1.6 ± 1.3
AUCK	174.83°E, 36.60°S	−0.8 ± 0.2(−1.8)	−0.4 ± 0.2(0.5)	−1.7 ± 1.0	0.3 ± 0.6
DARW	131.13°E, 12.84°S	−2.7 ± 1.2(−4.1)	−3.5 ± 1.3(−2.5)	−0.6 ± 1.0	1.9 ± 0.4
HOB2	147.44°E, 42.81°S	1.8 ± 0.4(1.0)	1.0 ± 02 (2.1)	0.2 ± 1.0	1.0 ± 0.7
KARR	117.10°E, 20.98°S	4.4 ± 1.5(4.0)	2.4 ± 3.8 (3.7)	−0.1 ± 3.0	1.5 ± 1.2
KOUC	164.29°E, 20.56°S	0.0 ± 0.2(−1.0)	0.0 ± 0.2 (1.0)		
LPIL	167.26°E, 20.92°S	−1.0 ± 0.3(−2.0)	−0.9 ± 0.2 (1.1)		
NOUM	166.41°E, 22.27°S	0.0 ± 0.4(−1.0)	0.0 ± 0.3 (1.0)	−1.9 ± 1.0	0.2 ± 0.5
SUVA	178.43°E, 18.15°S	−0.9 ± 1.9(−1.9)	0.6 ± 1.4 (1.9)		
TID2	148.98°E, 35.40°S	1.7 ± 0.4(0.9)	0.2 ± 0.3 (1.3)	2.4 ± 1.0	2.0 ± 0.6
TOW2	147.06°E, 19.27°S	1.1 ± 0.6(0.2)	−1.6 ± 0.6(−0.5)	1.0 ± 1.0	1.7 ± 0.4
YAR1	115.35°E, 29.05°S	0.0 ± 0.5(−1.4)	0.0 ± 0.5(−1.7)	0.9 ± 3.0	0.2 ± 1.6
		Pacific Plate			
CHAT	183.43°E 43.96°S	−1.2 ± 0.3(−1.1)	0.6 ± 0.3(2.3)	−0.1 ± 1.0	0.7 ± 0.7
FALE	188.00°E 13.83°S	1.3 ± 2.0(0.2)	−1.9 ± 0.8(−0.7)		
FTNA	181.88°E 14.31°S	1.9 ± 0.9(1.9)	−1.2 ± 0.5(−0.2)		
KOKB	200.34°E 22.13°N	0.7 ± 1.1(0.7)	−1.1 ± 0.7(−0.2)	−0.6 ± 1.0	0.5 ± 0.5
KWJ1	167.73°E 8.72°N	−1.4 ± 0.9(−1.4)	−0.3 ± 0.5(0.7)	−1.4 ± 1.0	0.3 ± 0.3
MARC	153.98°E 24.29°N	−1.4 ± 2.5(−2.8)	7.6 ± 2.4(8.7)		
OUSD	170.51°E 45.87°S	2.0 ± 0.4(2.1)	1.2 ± 0.5(2.6)		
THTI	210.39°E 17.58°S	3.0 ± 1.6(2.1)	−2.1 ± 1.2(−0.4)	2.9 ± 1.5	−0.1 ± 1.2

5 mm for horizontal components and around 15 mm for the vertical components. It is worth comparing results from the colocated temporary and permanent pairs of sites in NC: KOUC and KOUM, LFOU and LPIL, and NOUM and TIND. KOUM, LFOU, and TIND are roving sites used prior to the installation of the CGPS network in NC, respectively sites KOUC, LPIL, and NOUM. After the CGPS sites were installed, KOUM, LFOU, and TIND were rarely occupied. Their time series extends much longer than the CGPS time series and they are strongly constrained by results obtained for computations where LPIL, KOUC, and NOUM are not present. That the velocities obtained for these sites are very close to those obtained for the corresponding CGPS sites over shorter time windows (the largest discrepancy is 1.3 mm/yr in horizontal velocity between LPIL and LFOU) is an indicator of the overall robustness of the velocity data set derived from the time series.

[10] In the procedure to determine reference positions and velocities, it was assumed that the site moved with a constant velocity. However, some sites within our network underwent coseismic steps. In such cases, a Heaviside function at the time of each event was added to the model fitting the series when the coseismic step was expected to exceed a few millimeters. The earthquakes involved are the Aneytum event (M_w = 6.9 in January 1994), the Malekula event (M_w = 7.3 in July 1994), the Walpole event (M_w = 7.5 in May 1995), the Ambrym event (M_w = 7.5 in November 1999), and the Santo event in October 2000 (M_w = 6.9). Preliminary results related to the sparsely surveyed Malekula and Walpole events were analyzed by *Calmant et al.* [1997] and *Calmant et al.* [2000], respectively. The 26 November 1999 Ambrym earthquake generated meter to centimeter level displacements at all sites in Central Vanuatu. *Pelletier et al.* [2000] report field observations of the ground motions related to this event.

3. Results and Discussion

[11] Convergence rates across the trench cannot be fully determined by computing a pole of relative motion constrained by magnetic anomalies and slip vectors. Indeed, numerous spreading axes and transform faults, for which motions are only approximately known, split the overriding NFB into platelets (Figure 1). A first estimate of convergence velocity near 20°S was published by *Dubois et al.* [1977] using the shape of the bulge of the plunging plate. *Pelletier et al.* [1998] integrated some GPS data with marine geophysical data and seismicity to propose an updated tectonic scheme for the North Fiji and Lau Basins. In the following section, we present a refined view of the convergence variations along the NH trench. Yet because tectonics of the NH arc are much visible in a reference frame where NFB is fixed, rather than relative to a fixed subducting Australian plate, we present in a second section the determination of a WNFB reference frame and the respective GPS-based motions.

3.1. Convergence at the NH Trench: Evidence for Along Strike Variations

[12] Along the NH subduction zone, the Australian plate subducts eastward beneath the Vanuatu arc. The convergence velocities derived by GPS in the present study are reported in Table 3 and Figure 4. Large variations in both the azimuth and modulus of the vectors are observed. The highest convergence (124 mm/yr) is found at TANA while the lowest (28 mm/yr) is found at SWBY and TNMR on Malekula. Lower rates, at sites VMVS (17.3 mm/yr) and LVMP (26.6 mm/yr), also on Malekula, are derived with large uncertainties and need further observations to be confirmed. Along the study area, vectors for the A/P convergence motion vary little. For instance, the NUVEL1-A model [*De Mets et al.*, 1994] predicts from 89 mm/yr, oriented N240°, at latitude 13°S to 74 mm/yr, N242°, at latitude 22.5°S. Therefore observed convergence variations are not related to the position of the A/P pole but rather to local tectonic processes. Based on observed convergence variations, the NH arc can be split into four segments identified geographically: northern, central, southern, and southernmost.

[13] In the northern segment (Banks and Torres sites), observed convergence is 65–75 mm/yr, very close to values predicted by A/P. At the central segment, including all the islands that surround the Aoba Basin, convergence is much lower than A/P: 28–42 mm/yr along the western island belt (Santo, Malekula) and 55 mm/yr along the eastern belt (Maewo, Pentecost), all trending southwestward. The lowest convergence velocities, from 28 to 31 mm/yr, characterize the sites closest to the NH plate boundary along the western coasts of Santo and Malekula. Along the southern segment, from Epi (16.5°S) to Aneytum (20°S), convergence regularly increases southward, equaling then exceeding A/P. Observed values range from ~60 mm/yr at North Epi to ~120 mm/yr at Tanna and Aneytum. The observed velocity at Futuna-Iti (FTNV) notably departs from this trend given its value, 95 mm/yr, and location, East of Tanna. In the southernmost segment, at latitudes south of 21°S, convergence departs from A/P in both rate (lower values) and azimuth (trending more southward).

[14] Another point highlighted by this data set is that convergence vectors are nearly always normal to the trench axis and parallel to the slip vector of major thrust-type earthquakes related to the subduction of the Australian plate all along the NH Trench (Figure 4). This is particularly notable at the southern virgation of the trench where GPS vectors trend N197° and N177°, respectively, at Matthew (MTTW) and Hunter (HUNT) while trending N248° and N249°, respectively, at Aneytum (YTUM) and Tanna (TANA). The most dramatic changes in convergence vectors occur where an aseismic ridge born by the Australian plate is subducting. First, at 15.7°S, the subduction of the DER is associated with reduced convergence at all the islands surrounding the Aoba Basin compared to rates found north and south of the collision area. Second, at 22°S, the LR enters the trench and collides with the arc. North of this collision area, convergence rates are the highest observed along the arc: 118 mm/yr at Aneytum (YTUM) and 124 mm/yr at Tanna (TANA). South of this collision area, much lower rates are found: 48 mm/yr at Matthew (MTTW) and 42 mm/yr at Hunter (HUNT).

3.2. Motions Relative to the NFB: Evidence for Arc Segmentation and Block Rotations

[15] The NH arc is separated from the Pacific plate by the NFB. In addition to the active boundaries between the NH platform and the NFB seafloor, other active structures split

Table 3. Global Positioning System-Derived Velocity at Vanuatu Sites Relative to the Australian Plate and to the Western North Fiji Basin[a]

Island	Site Location	Name	Velocity Relative to the Australian Plate, mm/yr	Velocity Relative to the Western NFB, mm/yr	Number of Campaigns	Time Window
			Northern Segment			
Torres	166.64°E, 13.33°S	TORS	64.8 ± 4.8 N254° ± 3°	25.1 ± 4.6 N101° ± 8°	4	1997–1999
Banks	167.72°E 13.67°S	MOTA	76.3 ± 3.6 N266° ± 2°	15.0 ± 3.8 N050° ± 14°	5	1997–1999
			Central Segment			
Maewo	168.08°E, 15.08°S	MAWO	57.2 ± 0.9 N253° ± 1°	33.9 ± 0.8 N092° ± 2°	7	1992–1999/1999–2000
Santo	166.82°E, 15.16°S	BIGB	37.6 ± 4.4 N248° ± 5°	54.3 ± 4.5 N090° ± 3°	6	1997–1999/1999–2000/2000–2000
	167.10°E, 15.13°S	HOGB	42.5 ± 2.0 N257° ± 3°	47.7 ± 2.0 N085° ± 3°	10	1997–1999/1999–2000/2000–2001
	166.66°E, 15.36°S	WUSI	29.5 ± 1.3 N253° ± 3°	62.1 ± 1.3 N086° ± 1°	6	1997–1999/1999–2000/2000–2001
	167.20°E, 15.45°S	**SANC**	**37.7 ± 0.5 N245° ± 1°**	**55.8 ± 0.5 N093° ± 1°**	**CGPS**	**1996–1999/1999–2000/2000–2001**
	166.77°E, 15.63°S	LISB	31.4 ± 1.9 N244° ± 4°	62.0 ± 1.5 N090° ± 2°	7	1992–1994/1994–1999/1999–2000/2000–2001
	167.09°E, 15.60°S	RATA	38.5 ± 2.2 N242° ± 4°	56.0 ± 1.6 N095° ± 3°	8	1992–1994/1994–1999/1999–2000/2000–2001
	166.90°E, 15.61°S	TASM	34.7 ± 1.5 N238° ± 3°	59.9 ± 1.1 N095° ± 1°	10	1992–1994/1994–1999/1999–2000/2000–2001
Aoba	167.68°E, 15.42°S	AOBA	40.5 ± 3.4 N260° ± 3°	50.6 ± 3.5 N082° ± 2°	6	1997–1999/1999–2000
Malo	167.25°E, 15.72°S	MALO	34.6 ± 5.4 N246° ± 7°	58.7 ± 5.4 N090° ± 3°	5	1997–1999/1999–2000/2000–2001
Pentecost	168.16°E, 15.48°S	PNCT	55.1 ± 1.6 N260° ± 1°	35.9 ± 1.6 N080° ± 2°	7	1992–1994/1994–1999/1999–2000
Malekula	167.17°E, 16.01°S	TNMR	28.3 ± 2.5 N249° ± 8°	63.6 ± 1.8 N086° ± 3°	6	1997–1999/1999–2001
	167.37°E, 15.99°S	WLRN	29.1 ± 1.2 N258° ± 4°	62.3 ± 1.2 N082° ± 2°	11	1996–1999/1999–2001
	167.56°E, 16.21°S	RNSR	30.8 ± 3.6 N256° ± 4°	60.5 ± 3.6 N084° ± 2°	12	1998–1999/1999–2001
	167.24°E, 16.16°S	LVMP	26.6 ± 13.1 N263° ± 15°	64.6 ± 13.1 N081° ± 6°	5	1998–1999/1999–2001
	167.39°E, 16.17°S	LMBU	29.8 ± 4.1 N257° ± 6°	62.3 ± 4.1 N083° ± 3°	6	1997–1999/1999–2001
	167.78°E, 16.45°S	MLKL	41.8 ± 1.7 N248° ± 2°	52.3 ± 2.0 N092° ± 2°	12	1992–1994/1994–1999/1999–2001
	167.45°E, 16.48°S	SWBY	28.4 ± 2.5 N255° ± 4°	63.7 ± 2.4 N085° ± 2°	9	1996–1999/1999–2000
	167.38°E, 16.23°S	VMVS	17.3 ± 8.8 N227° ± 29°	78.3 ± 8.1 N089° ± 6°	3	1999–2001
Ambrym	167.92°E, 16.26°S	AMBR	32.4 ± 5.3 N239° ± 7°	63.2 ± 5.5 N091° ± 3°	9	1996–1999/1999–2001
			Shepperd Segment			
Epi	168.16°E, 16.60°S	NEPI	57.7 ± 12.2 N232° ± 10°	50.2 ± 12.9 N115° ± 7°	7	1997–1999/1999–2000
	168.28°E, 16.80°S	VOTL	71.2 ± 1.9 N235° ± 2°	41.6 ± 1.1 N127° ± 2°	5	1996–1999/1999–1999
	168.36°E, 16.83°S	NAMU	69.3 ± 7.3 N230° ± 6°	48.3 ± 4.4 N127° ± 6°	2	1999–2001
Tongoa	168.53°E, 16.92°S	TGOA	77.8 ± 2.4 N250° ± 3°	20.6 ± 1.7 N121° ± 7°	5	1997–1999/1999–1999
Emae	168.37°E, 17.05°S	EMAE	77.5 ± 6.6 N243° ± 4°	29.6 ± 3.6 N133° ± 7°	4	1997–1999/1999–1999
Nguna	168.33°E, 17.43°S	UTAN	83.1 ± 1.2 N245° ± 1°	25.5 ± 1.5 N140° ± 3°	4	1997–2001
Efate	168.20°E, 17.64°S	MGAL	85.5 ± 3.6 N247° ± 1°	22.3 ± 2.3 N145° ± 8°	4	1997–2001
	168.32°E, 17.73°S	**VILA**	**89.3 ± 0.3 N246° ± 1°**	**23.8 ± 0.5 N152° ± 1°**	**CGPS**	**1996–2001**
	168.56°E, 17.78°S	EFAT	94.0 ± 1.0 N245° ± 1°	24.7 ± 1.6 N163° ± 2°	18	1990–1994/1994–2001
			Southern Segment			
Erromango	169.02°E, 18.82°S	DILB	117.7 ± 1.7 N247° ± 1°	33.0 ± 1.4 N207° ± 3°	4	1996–1999
Aniwa	169.60°E, 19.24°S	ANIW	116.2 ± 3.3 N246° ± 1°	31.9 ± 2.8 N203° ± 6°	3	1997–1999
Tanna	169.25°E, 19.53°S	TANA	123.8 ± 1.3 N249° ± 1°	35.3 ± 1.7 N218° ± 2°	19	1992–1994/1994–1995/1995–1999
Aneytum	169.77°E, 20.14°S	YTUM	118.0 ± 2.1 N248° ± 1°	29.8 ± 2.0 N211° ± 4°	4	1997–1999
			Southernmost Segment			
Matthew	171.36°E, 22.34°S	MTTW	48.1 ± 2.4 N197° ± 6°	87.3 ± 5.1 N108° ± 2°	11	1992–1995/1995–2000
Hunter	172.09°E, 22.40°S	HUNT	42.3 ± 11.8 N177° ± 30°	101.3 ± 22 N102° ± 7°	4	1997–2000
			WNFB			
Futuna-iti	170.23°E, 19.52°S	FTNV	95.7 ± 1.1 N259° ± 1°	[b]0.6 ± 1.3 N031° ± 116°	4	1996–1999

[a]A "/" indicates that the time series was interrupted by a coseismic step that year. Continuous Global Positioning System sites are typeset in bold; their data have been grouped into 10-day sessions.
[b]Velocity at Futuna-Iti relative to WNFB is minimum by construction.

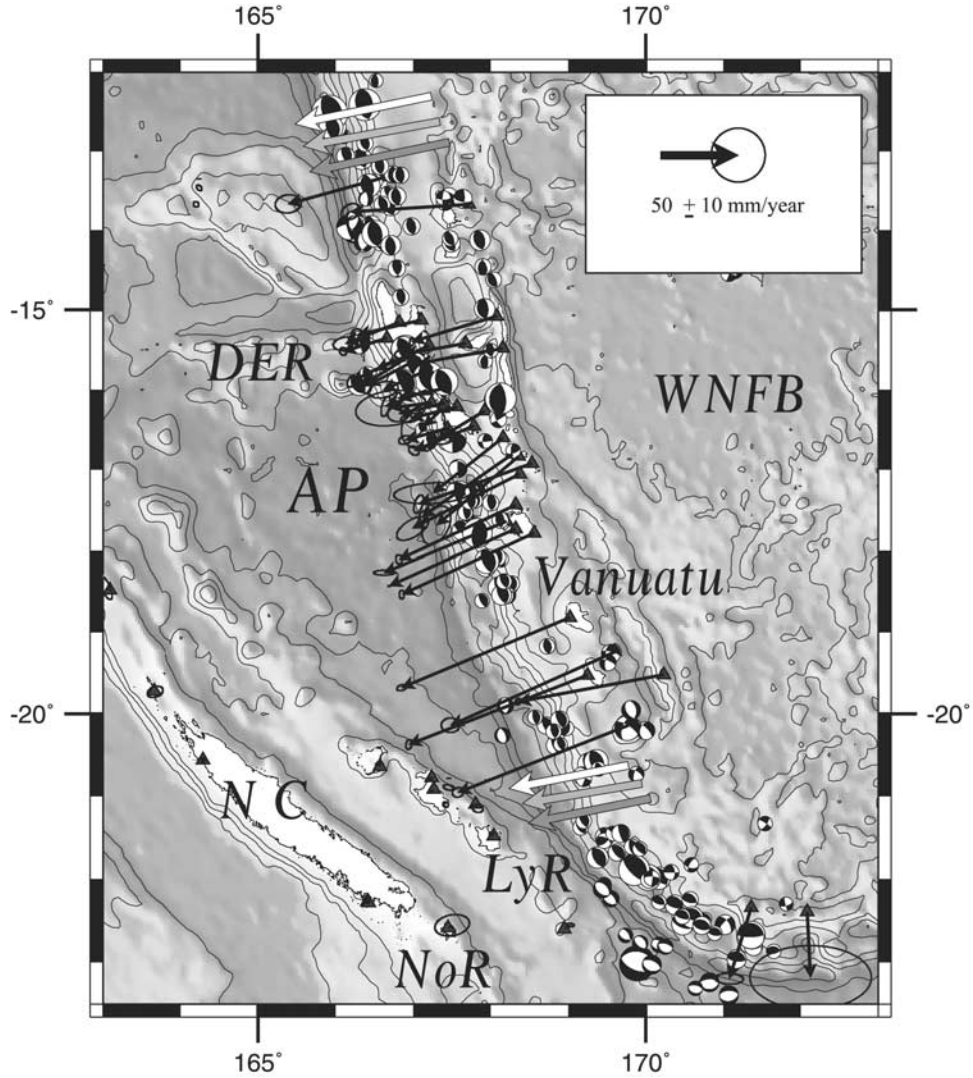

Figure 4. GPS convergence vectors across the New Hebrides subduction zone in an Australia-fixed reference frame. Large arrows show A/P motion derived in this study (white), derived from NUVEL-1A (light gray), and derived from Tregoning 2002 (dark gray). Labels: DER, D'Entrecasteaux Ridge; NC, New Caledonia; LyR, Loyalty Ridge; and NoR, Norfolk Ridge. See color version of this figure in the HTML.

the NFB into a jigsaw of platelets between the NH arc and the Pacific plate (Figure 1). Our GPS data set includes two sites, FTNV and FTNA, located on such platelets. FTNV is set on Futuna-Iti Island, located at 170°E, 19.5°S on the eastern rim of the Futuna Trough (Figure 5). Its motion relative to the Pacific plate is 17 mm/yr oriented N257°.

[16] FTNA is set on Futuna-Nui Island (not to be confused with the aforementioned island of Futuna-Iti) which lies south of the Vitiaz Trench Lineament in the northeast part of the NFB (see location in Figures 1 and 3). It is commonly assumed that no motion presently occurs across along the Vitiaz Trench Lineament, a fossil subduction zone. The NFB seafloor lying south of the Vitiaz Trench Lineament is bounded in the south by the Hazel Holme ridge (HHR). This E-W trending feature is described by *Pelletier et al.* [1988] and *Louat and Pelletier* [1989] as an extensional feature or a very slow spreading center. It extends eastward toward the South Pandora ridge, also recognized as a slow spreading center [*Price and Kroenke*, 1991; *Lagabrielle et al.*, 1996] and abuts in the West in the NH platform at 13.6°S. The velocity of FTNA with respect to the pole-predicted velocity of the Pacific plate is 2.2 ± 0.8 mm/yr while the velocity of FALE, a nearby CGPS site in Samoa which is actually on the Pacific plate, is 2.3 ± 1.2 mm/yr. This result strongly suggests that Futuna-Nui does indeed move in unison with the Pacific plate, as does the whole platelet between the Vitiaz Trench and the HHR. *Louat and Pelletier* [1989] proposed that the extension in the HHR trends N25° and the inferred motion of divergence, vanishing westward, should not exceed 20 mm/yr. A N-S divergence of 15 mm/yr is proposed along the South Pandora Ridge further east [*Lagabrielle et al.*, 1996]. At 18.5°S, another E-W trending feature named the West Spreading ridge (WSR) is interpreted as an active spreading ridge that crosscuts the western NFB [*Pelletier et al.*, 1998]. The divergence rate of this feature is unknown. The WSR abuts the NH platform east of Erromango Island and separates the southern NH back arc troughs into two domains: the Efate

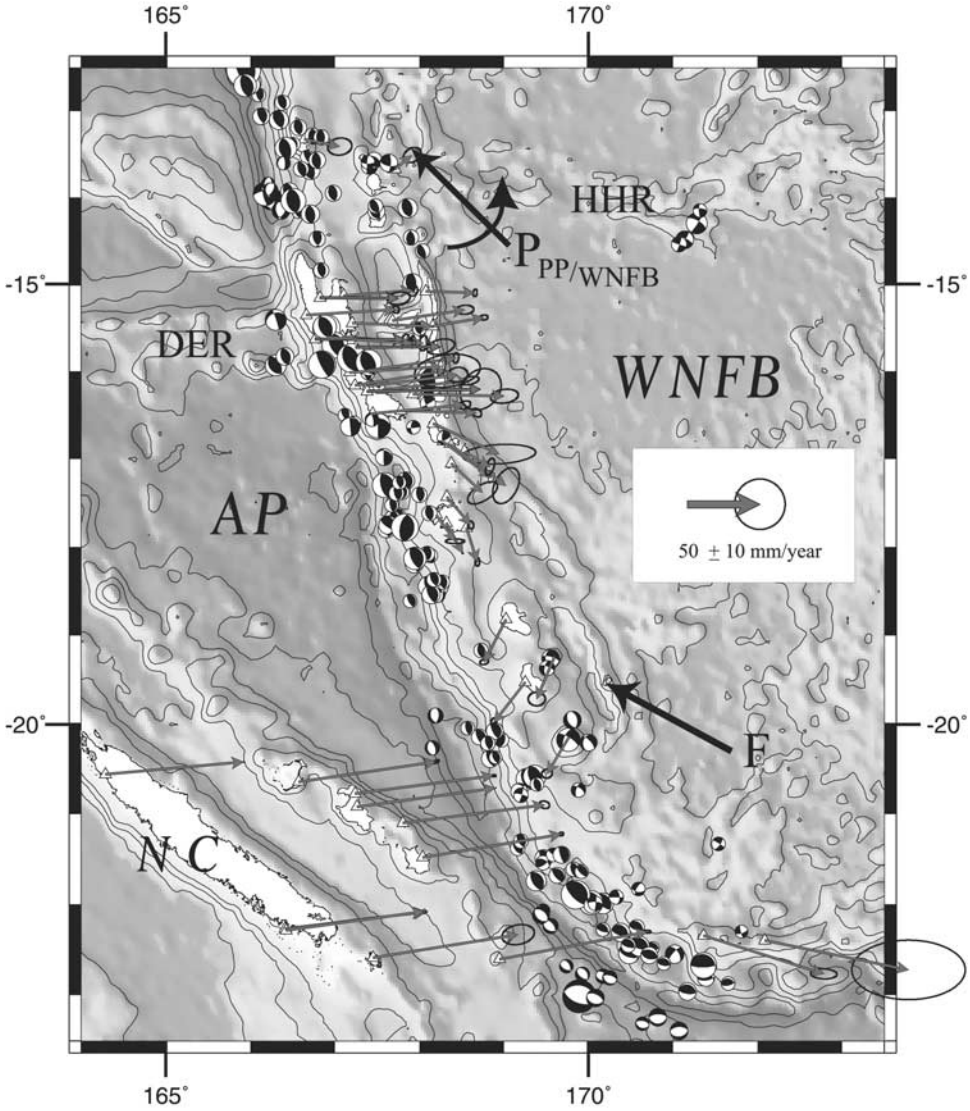

Figure 5. GPS vectors relative to the western North Fiji Basin (WNFB). Labels: DER, D'Entrecasteaux Ridge; NC, New Caledonia; HHR, Halzel Holme Ridge; F, Futuna-Iti; $P_{PP/WNFB}$, hypothesized location of the pole of WNFB/Pacific relative motion. See color version of this figure in the HTML.

Trough in the north and the Erromango-Futuna Trough in the south [*Pelletier et al.*, 1998]. Futuna-Iti lies on the platelet south of the WSR. The slow, southwestward motion of Futuna-Iti relative to the Pacific plate confirms that the HHR and WSR features together spread mostly NE-SW and that their total divergence should not exceed 20 mm/yr. Moreover, it suggests that spreading is very slow at the WSR. Thus the different platelets that border the NH platform on the east from the Torres Islands in the north to Aneytum in the south will be considered hereafter as a single unit in terms of kinematics, namely the WNFB reference. The motion of the WNFB relative to the Pacific plate was modeled by a plane rotation, $\Omega_{WNFB/P}$, derived empirically. The location of the pole was fixed where the HHR abuts in the NH margin and where extension vanishes, at 13.5°S and 167.5°E. The rotation rate was determined such that it predicts both the motion at Futuna-Iti relative to the Pacific plate (17 mm/yr) and extension along the HHR. Accordingly, the rate is 1.10°/Ma.

[17] Motions of the GPS sites in Vanuatu relative to the WNFB plate were derived by removing the velocity predicted by $\Omega_P + \Omega_{WNFB/P}$ from the initial velocity field determined in the ITRF 2000 reference frame. These motions are reported in Table 3 and displayed in Figure 5. It is worth noting that the small residual at FTNV implies that the azimuth of the motion at Futuna-Iti is well accounted for by $\Omega_{WNFB/P}$, although the latter's pole was fixed using tectonic considerations only.

[18] GPS velocities along the NH arc relative to the WNFB show large variations. In the northern segment, reduced motions (less than 25 mm/yr) are found. In the central segment, larger (35–65 mm/yr) eastward motions are derived. In the southern segment, the vector azimuth progressively turns from southeastward to south-southwestward. South of 22°S, in the southernmost segment, motion is large (~90 mm/yr) and trends east-southeastward, which is opposite in direction from that observed north of 22°S.

Table 4. Euler Poles Fitting the Site Motions on the Vanuatu Platform With Respect to the Western North Fiji Basin[a]

	Ω	Latitude of Pole	Longitude of Pole
Ω_S	6.29 ± 0.3 (−)	18.39° ± 0.06°S	166.56° ± 0.1°E
Ω_N	10.16 ± 0.6 (+)	14.52° ± 0.12°S	166.91° ± 0.06°E
$\Omega_C = \Omega_N + \Omega_S$	3.9 ± 0.5 (+)	8.26° ± 1°S	167.44° ± 0.07°E

[a]Unit is °/Ma. Sites of Matthew and Hunter (southernmost segment) are excluded from the data set used in the least squares fit. The minus sign signifies clockwise rotation; the positive sign signifies counterclockwise rotation.

[19] Due to the progressive rotation of vectors from 15° to 21°S, we attempted to least square fit this data subset by a single rotation. The corresponding Euler pole is centered southwest of Efate and rotates clockwise at a rate of 10.4°/Ma. However, this model produced large residuals between observed and predicted vectors, suggesting that the eastward vectors in Central Vanuatu are too large with respect to the vectors in the south for a single rotation to fit. A more refined model was therefore computed. First pole was fitted to the data in the southern and central segments, and the second pole fitting the data in the northern and central arc segments. The first pole produced by this two-pole model, Ω_S, is described in Table 4 and is similar to the preliminary solution derived by the single-pole model described above, rotating clockwise, but with a slower rotation of 6.29°/Ma. The second pole produced by the two-pole model, Ω_N, turns counterclockwise and is located north of Santo. Motion of the Central Vanuatu sites is obtained by combining the rotations of both poles from the two-pole model since both poles are partly constrained by the data in this area. This leads to an Euler pole rotating counterclockwise and situated further north, at 8.3°S, 167.4°E (Euler pole Ω_C in

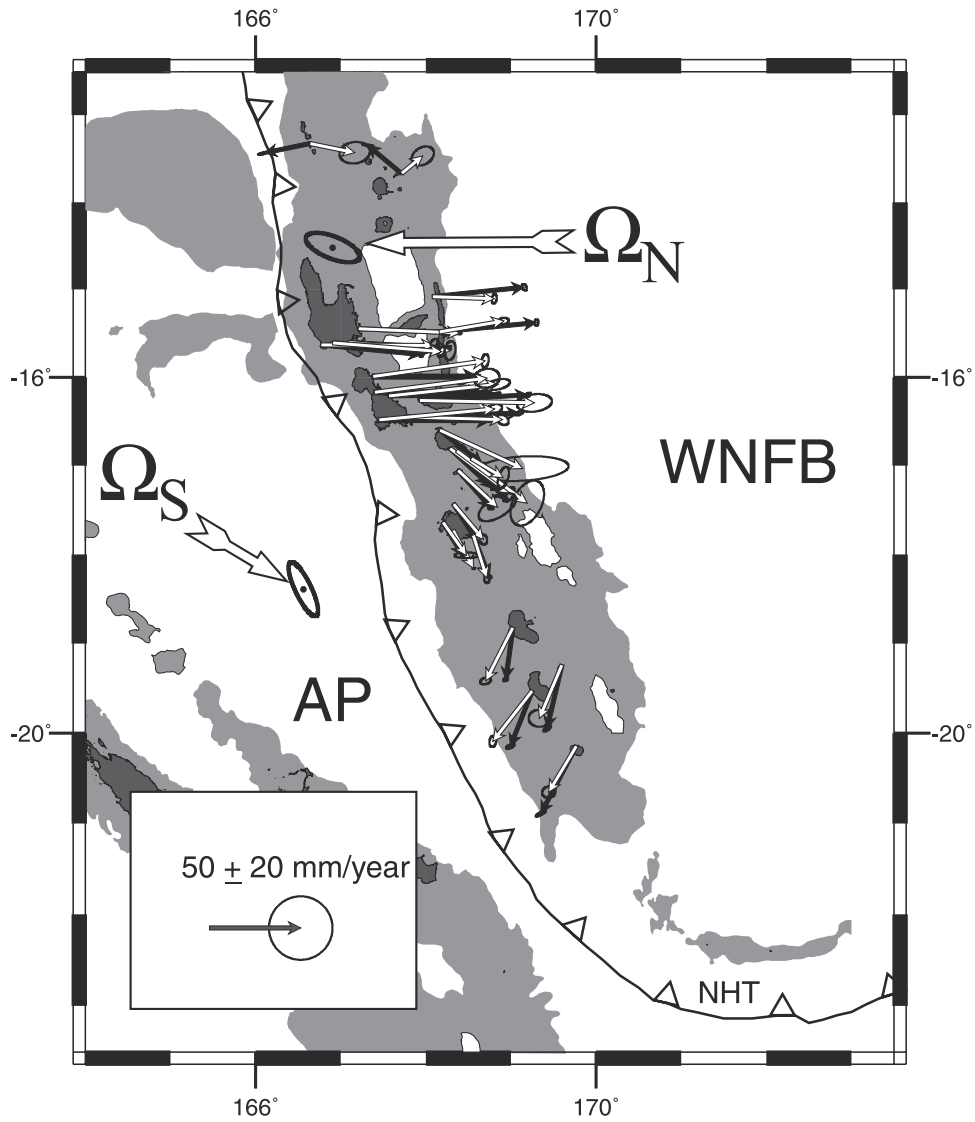

Figure 6. Observed (white arrows) and pole-derived (black arrows) vectors within the Vanuatu archipelago relative to the WNFB. For clarity, only a subset is shown for Central Vanuatu. Ellipses circling pole locations are 1σ uncertainties. Labels: AP, Australian plate; WNFB, western North Fiji Basin; and NHT, New Hebrides Trench.

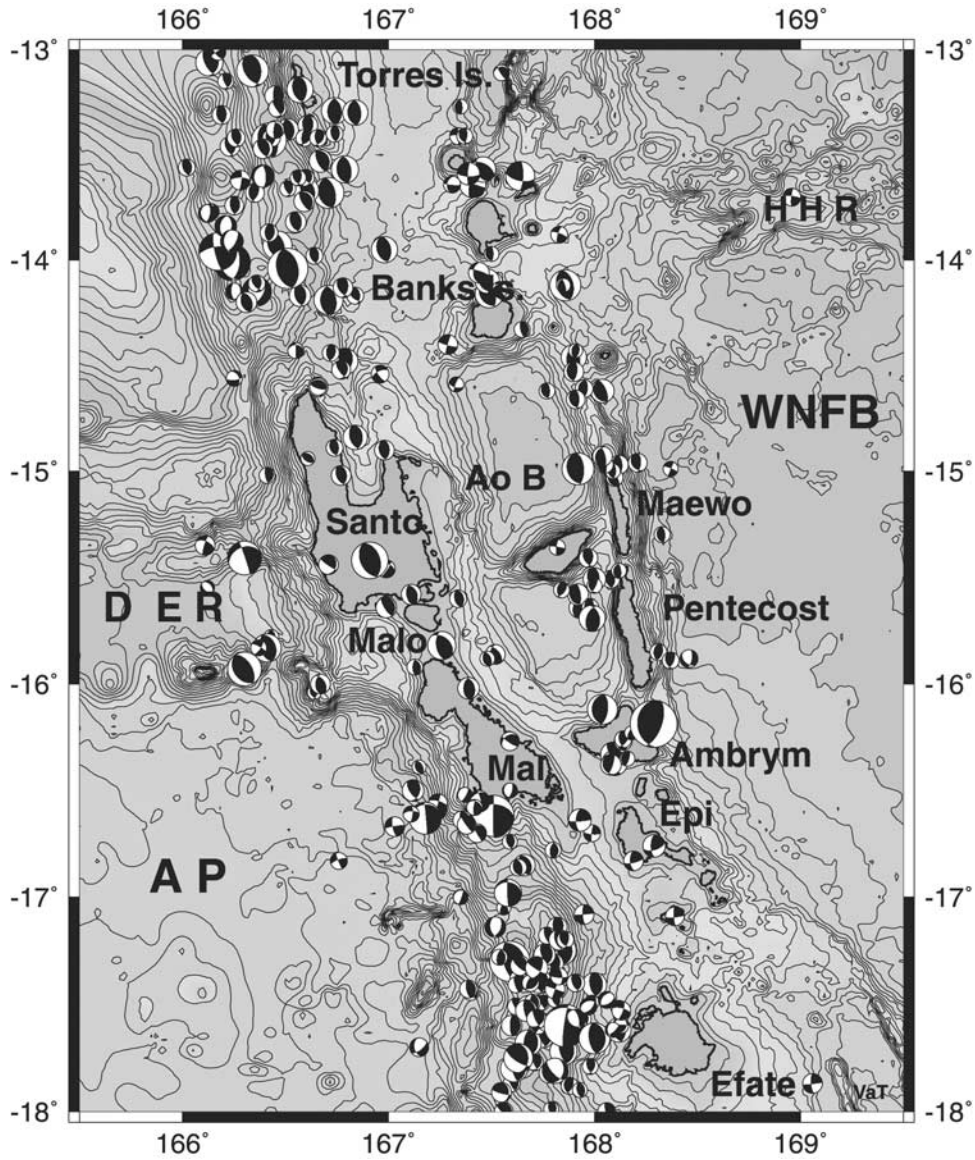

Figure 7. Bathymetric map of Central Vanuatu. Contour interval is 200 m. The central volcanic arc is marked by the Epi/Ambrym/Aoba and Banks Islands. The western belt islands (Malekula, Malo, Santo) reveal the uplift of the New Hebrides platform due to the collision of the D'Entecasteaux Ridge with the New Hebrides Trench. The eastern belt islands (Maewo, Pentecost) reveal seafloor uplift due to eastward back thrusting over the WNFB. Focal mechanism solutions are shown for shallow earthquakes (<50 km, Centroid Moment Tensor Solutions, location NEIC) for the period 1977–2002 (size of circles as function of magnitude of event, lower hemisphere projection). Labels: AP, Australian plate; DER, D'Entecasteaux Ridge; WNFB, western North Fiji Basin; AoB, Aoba Basin; HHR, Hazel Holmes Ridge; VaT, Vate Trough; and Mal, Malekula Island. See color version of this figure in the HTML.

Table 4). Due to this remote latitude, modeled motions throughout Central Vanuatu remain almost parallel, trending eastward. The RMS discrepancy between observed and modeled velocities (Figure 6) is 6 mm/yr and the unit covariance factor is 4.2. These statistics suggest that the current model is simplistic and that unmodeled effects contribute to the observed values. Indeed, strain accumulation is likely to affect the displacement rates in Central Vanuatu. It is also worth noting that the uneven distribution of velocity estimates (Ω_S is much better sampled than Ω_N) biases the relative contribution of the two poles in the total motions in Central Vanuatu (Ω_N is more constrained by the residuals in Central Vanuatu not accounted for by Ω_S than by the velocity estimates in the northern segment). The two-rotation model proposed in this study is therefore a first-order description of the kinematics of the Vanuatu Islands. According to this model, the NH arc, from Torres in the north to Aneytum in the south, is composed of three parts: a northern segment (north of 14°S), a central segment (from 14° to 16.5°S), and a southern segment (from 16.5° to 21°S). Note that these arc segments correspond geographically to

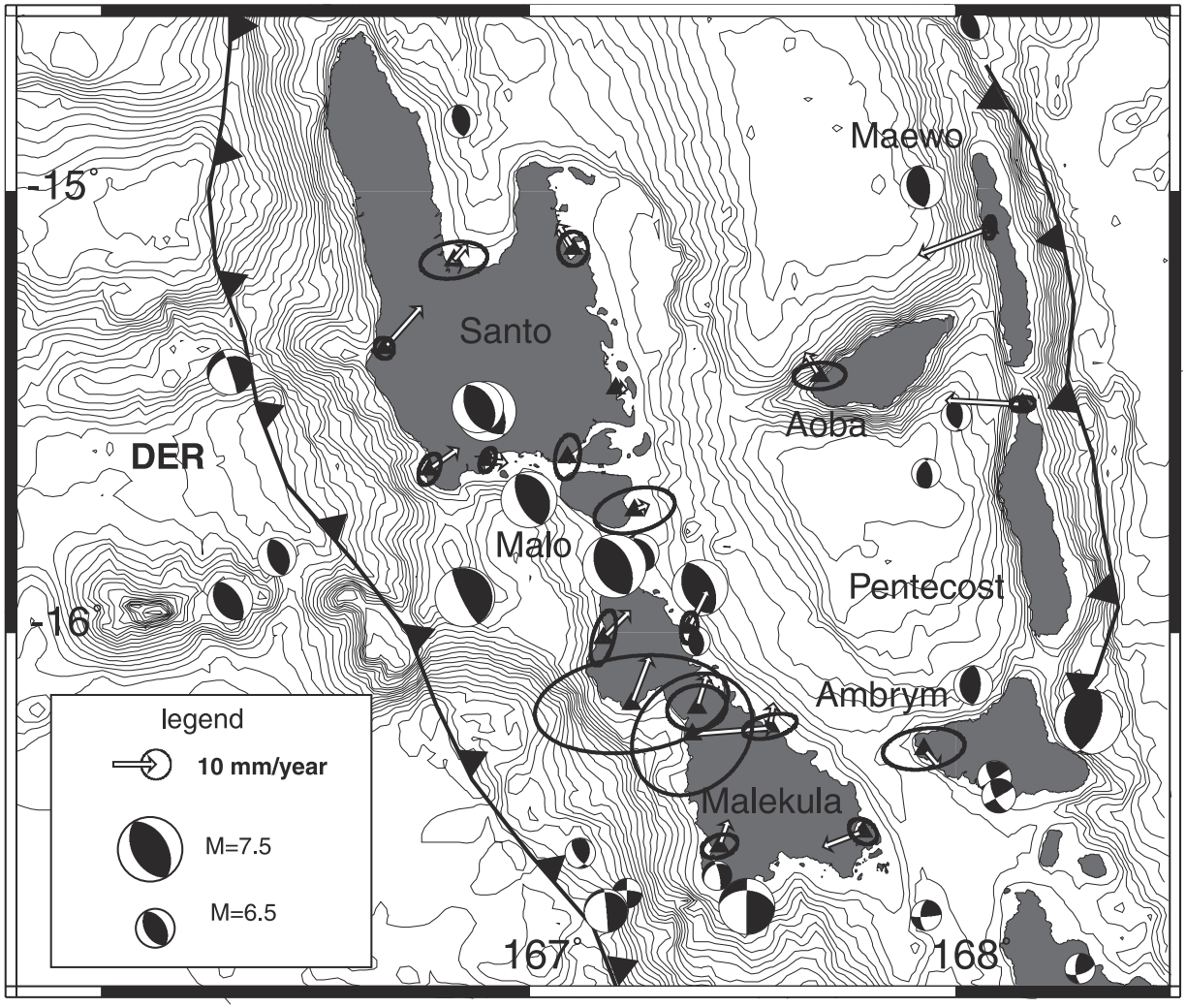

Figure 8. Velocity residuals (observed-modeled) in Central Vanuatu. Ellipses represent 2σ uncertainty levels for the GPS-derived vectors (uncertainties of modeled vectors are not considered). Focal mechanism solutions are from the CMTS Harvard catalog (M_w > 6.5, location CMTS, period 1977–2002) and from *Ebel* [1980] for the cluster of events related to the 1965 crisis between Santo and Malekula. For the Malekula event in 1994 and the Ambrym event in 1999, locations are from *Calmant et al.* [1997] and Regnier et al. (submitted manuscript, 2002), respectively. Size of circles as function of magnitude of event, lower hemisphere projection. Labels: DER, D'Entrecasteaux Ridge; AP, Australian plate; and BATB, Back Arc Thrust Belt.

the northern, central, and southern segments described in section 3.1.

3.3. Central Vanuatu: Evidence for Back Arc Shortening and Strain Accumulation

3.3.1. Back Arc Convergence

[20] Previous studies of seismicity [*Isacks et al.*, 1981; *Louat et al.*, 1988], neotectonics [*Taylor et al.*, 1980, 1987, 1990], marine geophysics [*Collot et al.*, 1985], kinematics [*Louat and Pelletier*, 1989], and geodesy [*Taylor et al.*, 1995] indicate in Central Vanuatu a very strong coupling between the overriding margin and the subducting plate as well as the presence of a back arc compressive belt. It has long been proposed that the reduced convergence at Central Vanuatu, together with other tectonic features such as the disappearance of the trench and uplift of the islands that bracket the Aoba Basin to the east and in the west (Figure 7), is a consequence of the presence of the DER on the Australian plate that opposes subduction [*Collot et al.*, 1985; *Taylor et al.*, 1995; *Pelletier et al.*, 1998; see also herein references]. Various crustal shortening rates have been estimated at the back arc, such as 36–83 mm/yr [*Taylor et al.*, 1995] and 40–60 mm/yr [*Pelletier et al.*, 1998]. The spatially dense network of GPS sites measured in the central arc and presented here allows us to establish the distribution of the convergence between the Australian plate, the central NH arc, and the NFB. According to Ω_C, the strain-free rate of convergence along the eastern back arc belt, referred to hereafter as the Back Arc Thrust Belt (BATB in Figure 8) increases slowly from 51 ± 2 mm/yr oriented N085° ± 2° at northern Maewo to 60 mm/yr oriented N087° ± 2° at eastern

Table 5. Residual (e.g., Difference Between Observed With Respect to Western North Fiji Basin and Ω_C-Derived) Velocities in Central Vanuatu

Island	Site Location	Name	Residual Velocity, mm/yr
	Western Island Belt		
Santo	166.82°E, 15.16°S	BIGB	4.8 ± 3.7 N040° ± 48°
	167.10°E, 15.13°S	HOGB	6.8 ± 2.2 N328° ± 17°
	166.66°E, 15.36°S	WUSI	13.3 ± 1.3 N042° ± 6°
	167.20°E, 15.45°S	**SANC**	**2.6 ± 0.5 N097° ± 7°**
	166.77°E, 15.63°S	LISB	8.5 ± 2.1 N055° ± 15°
	167.09°E, 15.60°S	RATA	1.6 ± 2.8 N161° ± 59°
	166.90°E, 15.61°S	TASM	4.7 ± 1.1 N097° ± 19°
Malo	167.25°E, 15.72°S	MALO	3.6 ± 5.4 N069° ± 62°
Malekula	167.17°E, 16.01°S	TNMR	8.9 ± 2.5 N045° ± 22°
	167.37°E, 15.99°S	WLRN	9.8 ± 2.0 N027° ± 8°
	167.56°E, 16.21°S	RNSR	5.5 ± 1.9 N008° ± 38°
	167.24°E, 16.16°S	LVMP	12.0 ± 8.5 N021° ± 62°
	167.39°E, 16.17°S	LMBU	8.1 ± 3.2 N017° ± 29°
	167.78°E, 16.45°S	MLKL	10.0 ± 1.7 N249° ± 9°
	167.45°E, 16.48°S	SWBY	6.5 ± 1.9 N019° ± 22°
	167.38°E, 16.23°S	VMVS	18.9 ± 8.2 N085° ± 25°
	Eastern Island Belt		
Maewo	168.08°E, 15.08°S	MAWO	17.7 ± 1.0 N249° ± 5°
Pentecost	168.16°E, 15.48°S	PNCT	18.0 ± 1.6 N273° ± 3°
	Central Islands		
Aoba	167.68°E, 15.42°S	AOBA	6.3 ± 2.3 N328° ± 28°
Ambrym	167.92°E, 16.26°S	AMBR	5.7 ± 3.7 N140° ± 42°

Ambrym. This exceeds the strain-free rate of convergence at the NH trench, which varies from 39 ± 2 mm/yr oriented N248° ± 3° to 31 ± 2 mm/yr oriented N250° ± 3° along the west coast of Santo and Malekula, respectively. This result suggests that a plate boundary jump is ongoing in the area facing the DER, and therefore the BATB must be regarded as the major tectonic element in the convergence process at Central Vanuatu with a reversal of the subduction polarity, although the absence of deep seismicity beneath the eastern island belt precludes this thrust being already a mature subduction zone (for an extended analysis, see Y. Lagabrielle et al., Coseismic and long-term vertical displacement due to back arc shortening, Central Vanuatu: An integrated analysis of field and marine data following the Mw 7.5, November 26th 1999, Ambrym earthquake, submitted to *Journal of Geophysical Research*, 2002; hereafter referred to as Lagabrielle et al., submitted manuscript, 2002).

3.3.2. Strain Accumulation

[21] In Central Vanuatu, observed rates at some sites significantly depart from values derived by fitted poles (Figure 8). These large residuals (Table 5) may result from unmodeled effects or erroneous assumptions in the data modeling (e.g., constant velocity throughout time, rigid block behavior of the segments). Besides, Ω_C was least squares fitted to a data set of uneven repartition and that presents significantly different values of uncertainties. The Ω_C is thus likely biased toward minimizing residuals on the western part of the network, where it is denser and where the smallest uncertainties are found (in particular at the CGPS site SANC).

[22] Given the historical occurrence of large (M_s > 7) earthquakes in this area, it is likely that some large residuals are partly caused by strain accumulation. If so, largest residuals should affect sites close to active boundaries, that is at the western and eastern borders of the area. Accordingly, sites located in the middle of the Aoba Basin should present small residuals. In fact, SANC, that likely constrained Ω_C noticeably and which motion is thus well fitted by this rotation, is situated on the eastern coast of Santo, where a potential lock of either interplate interface would generate only small rates of strain accumulation. The hypothesis according which the velocity data set may include interseismic strain is also supported by the fact that all the residuals larger than 10 mm/yr are located either on the west coast of the Santo and Malekula Islands or on the Maewo and Pentecost Islands of the eastern belt. Sites on Aoba and Ambrym Islands, whose central position suggests that they are not likely to undergo large interseismic strain, display residuals of ~6 mm/yr, but trending in opposite directions. Yet both are active volcanoes and volcanically induced deformation here cannot be fully discarded. Therefore owing to the E-W symmetry of the active boundaries that bracket Central Vanuatu and to the position of SANC, away from these boundaries, bias in Ω_C due to interseismic strain contribution to the observed velocities is not likely to introduce systematic errors in modeled velocities greater than the overall uncertainty of 4 mm/yr for Ω_C-derived velocities in Central Vanuatu.

[23] A striking feature displayed by these velocity residuals is that most trend toward the center of the Aoba Basin. This is consistent with other geological and geophysical observations that this basin undergoes compression due to its position between two main thrust boundaries [*Pelletier et al.*, 1994]. Focal mechanisms for major earthquakes recorded in Central Vanuatu since 1976 are shown in Figure 8. They can be split in two groups: thrust events related to subduction of the Australian plate along the NH trench and thrust events

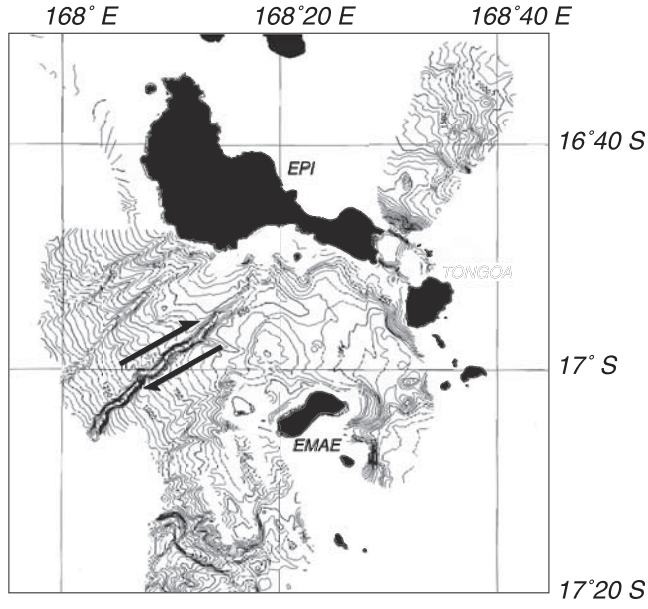

Figure 9. Multibeam bathymetry of part of the Shepperd area at the southern termination of the Back Arc Thrust Belt. Contour interval is 50 m. Data were acquired during the CALVA cruise [*Eissen et al.*, 1997]. Arrows indicate present shearing motion in the Shepperd area as derived from Euler poles for the southern and central segments.

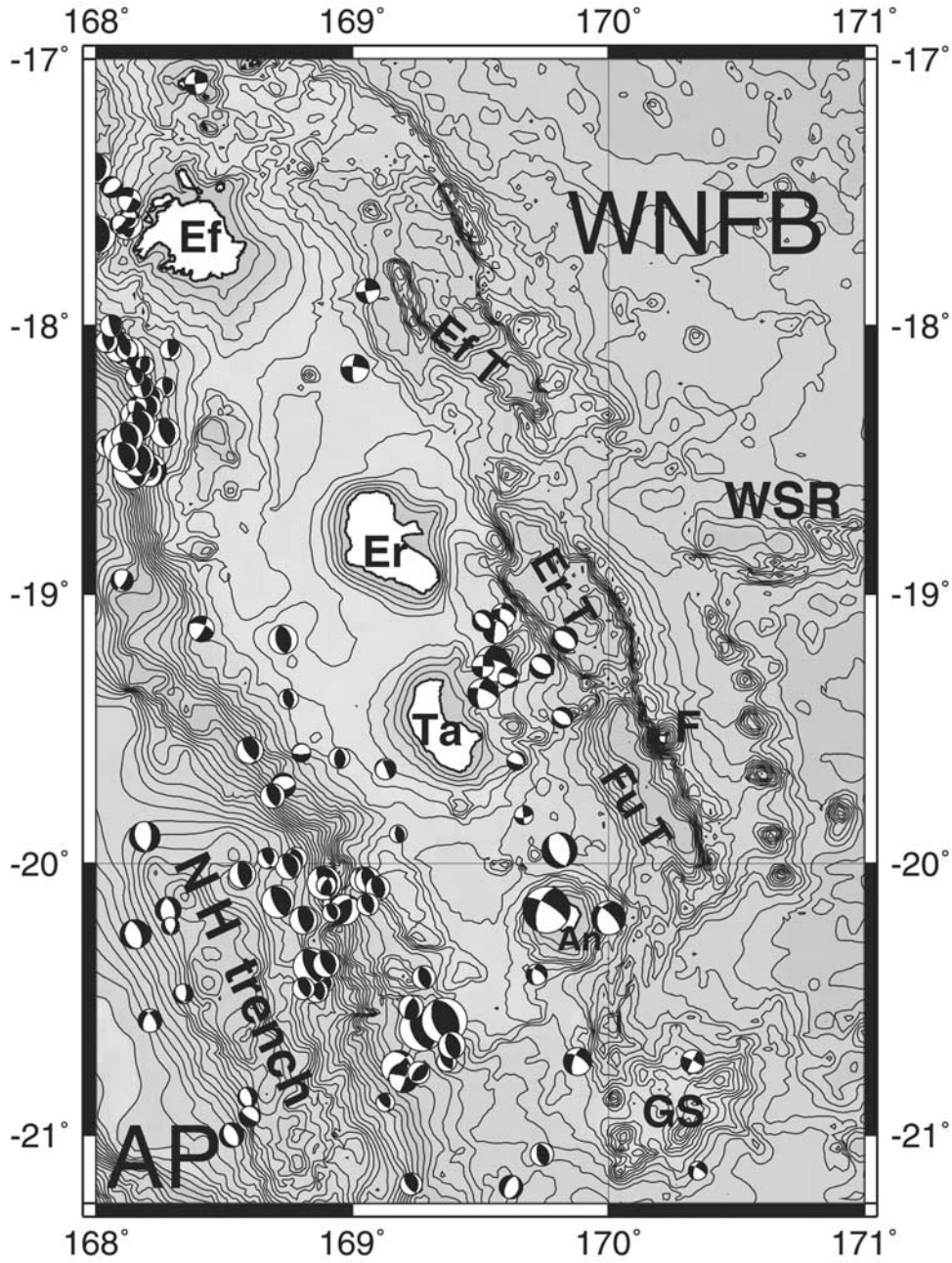

Figure 10. Bathymetric map of the southern segment of the New Hebrides subduction zone, including the southern back arc troughs. Contour interval is 200 m. Focal mechanism solutions are shown for shallow earthquakes (<50 km, Centroid Moment Tensor Solutions, location NEIC) for the period 1977–2002 (size of circles as function of magnitude of event, lower hemisphere projection). Southern back arc troughs include: EfT, Efate Trough; ErT, Erromango Trough; FuT, Futuna Trough; and AnT, Aneytum Trough. Labels: GS, Gemini Seamounts; WSR, Western Spreading Ridge; and WNFB, western North Fiji Basin. See color version of this figure in the HTML.

related to compression along the BATB. Epicenters are distributed throughout the islands of the western belt, indicating that the entire interface beneath Santo and Malekula has experienced a seismic rupture during the past four decades. As far as GPS sites on the west coast are concerned, residuals are large and the trend is roughly parallel to the direction of convergence and seismic slip motion. Thus although no accurate modeling of potential earthquakes can be performed using the present data set (too many residuals are still within uncertainties), it can be inferred that they globally indicate that the subduction interface is strongly coupled beneath Santo and Malekula, indicating a characteristic stick-slip seismic cycle.

[24] The residuals found at MAWO and PNCT are the most significant ones, far larger than associated uncertainties. They both trend eastward. Such a trend is consistent with a hypothesis of locking along the BATB interface, which plunges westward beneath Maewo and Pentecost

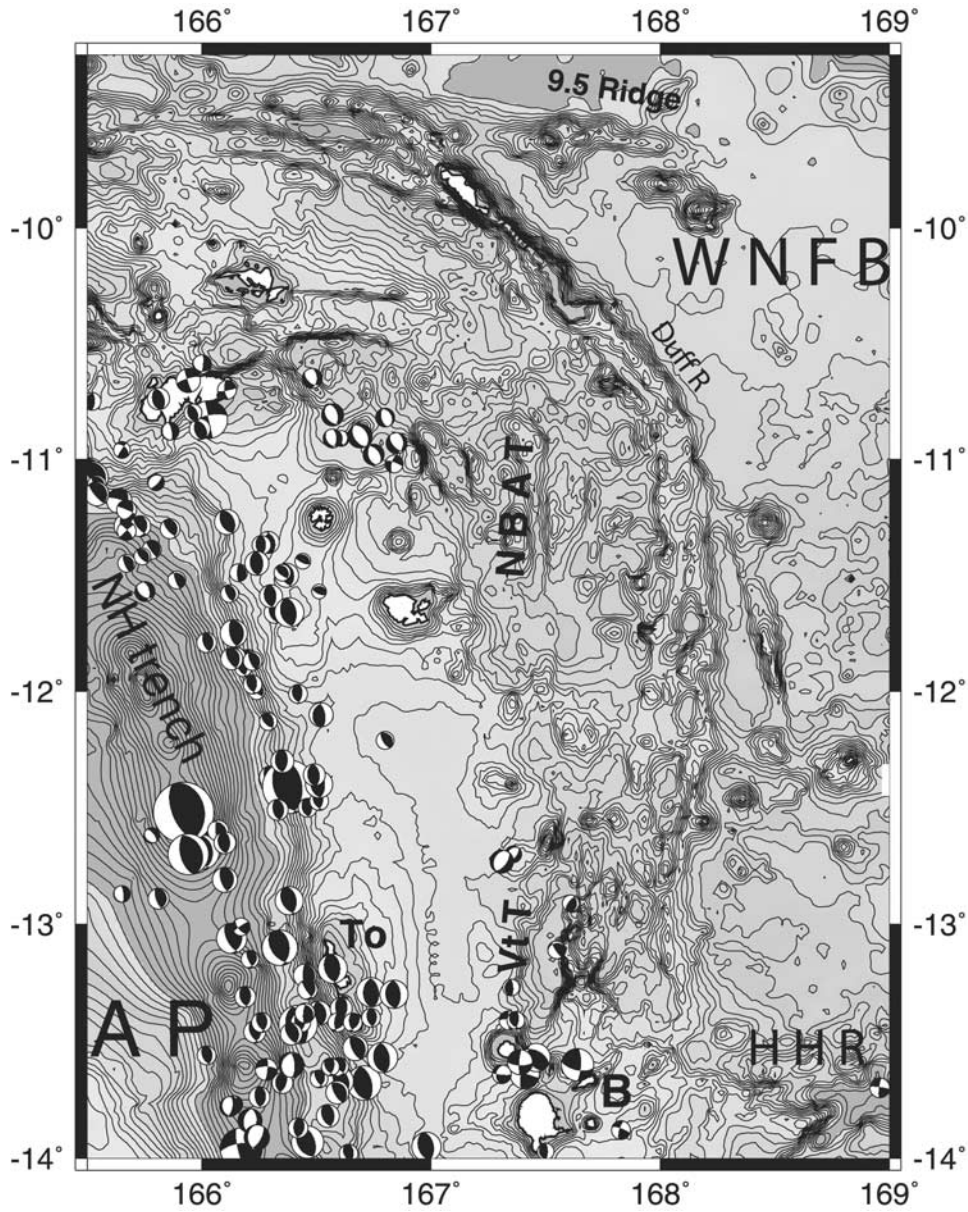

Figure 11. Bathymetric map of the northern segment of the New Hebrides subduction zone including the back arc troughs. Contour interval is 200 m. Focal mechanism solutions are shown for shallow earthquakes (<50 km, Centroid Moment Tensor Solutions, location NEIC) for the period 1977–2002 (size of circles as function of magnitude of event, lower hemisphere projection). Labels: AP, Australian plate; NBAT, Northern Back Arc Troughs; HHR, Hazel Holme Ridge; WNFB, western North Fiji Basin; B, Banks Islands; and To, Torres Islands. See color version of this figure in the HTML.

Islands. These residuals amount to ~18 mm/yr at both sites, which is approximately one-third of the potential deficit of slip velocity at the locked BATB, namely ~55 ± 5 mm/yr, predicted by Ω_C. This ratio is very large for such a tectonic context of oceanic thrusting. If confirmed, these residuals predict that large, shallow earthquakes are expected to unlock the Maewo/Pentecost part of the BATB. Yet no major earthquakes have ever been recorded in this part of the BABT. However, such was the case at the southern termination of the BATB (south Pentecost to Ambrym) until the Ambrym, M_w = 7.5, earthquake occurred in 1999 [*Pelletier et al.*, 2000; *Regnier et al.*, 2003]. Earthquakes beneath Maewo and north Pentecost that rupture this locked part of the BATB could resemble the Ambrym event.

3.4. Shepperd Area: A Transition Zone Accommodating the Shear Between the Central and Southern Segments

[25] The Shepperd area, bounded by Malekula and Ambrym to the north and by Efate to the south, constitutes the transition area between the southern and central arc segments. Vectors relative to the WNFB in the Shepperd area are oriented southeastward, intermediate between the eastward motion of the central block and toward SSE to

SSW motion found further south (Figure 5). The magnitude of vectors relative to the WNFB regularly decreases in this area, from 50 mm/yr north of Epi to ~25 mm/yr at Efate. Vector azimuths trend N115° to N160°. Accordingly, the pole Ω_S is located southwest of Efate (Table 4 and Figure 6). Because a pair of poles was necessary to describe the observed motions throughout the Vanuatu arc, some dextral shear has to be accommodated between the central and southern segments, that is, within the Shepperd area. Strike-slip fault-type focal mechanism solutions in this region show slip orientations trending from N050° to N090° (Figure 7). The pole-predicted right-lateral strike-slip motion is 51 ± 3 mm/yr oriented N060° ± 5°. This pole-derived orientation and the orientation of earthquake slip vectors are consistent with the strike of a series of submarine canyons revealed in bathymetry data (Figure 9), especially those collected southwest of Epi during the CALVA cruise aboard the N/O *l'Atalante* [*Eissen et al.*, 1997]. These canyons, running N050°, are interpreted as the surface expression of strike-slip faults across the NH platform that currently accommodate or formerly accommodated the shear between the central and southern segments. Moreover, the progressive southward rotation of the GPS vectors corresponds to changes in the structural direction of the Efate Trough, which trends NNW-SSE but is prolonged in the north by NW-SE and then WNW-ESE trending scarps where it abuts in the Shepperd Island area (Figure 7). Convergence at the southern tip of the BATB, extension at the northern tip of back arc troughs running east of Efate, and the aforementioned dextral strike-slip motion might join in a kind of triple junction around on 17°S, 168.5°E. It is worth noting that the Kuwae submarine volcano lying at this connection area produced one of the largest historical eruptions in 1420–1430 A.D. [*Monzier et al.*, 1994].

3.5. Southern Segment: Rapid Convergence, Clockwise Rotation, and Extension in the Back Arc Erromango-Futuna Trough

[26] The southern segment extends from Efate to Aneytum Islands. It is characterized by the highest rates of convergence (~120 mm/yr) relative to the Australian plate. This high convergence was recognized previously at Tanna [*Taylor et al.*, 1995; *Calmant et al.*, 1995, 2000]. It is regionally confirmed in this extended data set, where values exceeding the A/P vectors by 30–35 mm/yr southwestward are found for all these islands. *Pelletier et al.* [1998] showed that the difference between actual convergence and A/P implies that some extension should occur in the troughs at the rear of the southern NH arc. The Erromango-Futuna Trough is the southern part of this series of troughs that border the NH platform on the east (Figure 10). The nature, origin, and tectonic significance of these troughs are still debated [*Maillet et al.*, 1995], but it is agreed that these are extensional features [*Recy et al.*, 1986, 1990] characterized by normal fault-type focal mechanisms (Figure 10). Multibeam echo sounder surveys included in the bathymetry of Figure 10, partly conducted aboard R/V *Jean Charcot* [*Recy et al.*, 1986], revealed that extension in the Futuna Trough trends N040°, oblique with respect to the mean trend of the trough. These bathymetric data also show an asymmetry of the trough, with a major scarp along the eastern flank and tilted blocks along the western flank. This, together with the earthquake epicenters that are located west of the western flank of the trough, suggests that extension in the trough is accommodated along a major listric fault emerging along the eastern flank of the trough and dipping westward beneath the western flank. The Ω_S-derived extension rate across the Futuna Trough is 46 ± 1 mm/yr oriented N030° ± 2°. Thus the geodetic direction of motion and the direction of extension from focal mechanism solutions are in good agreement with marine geophysical data. Then, that extension which is oriented according to Ω_S small circles instead of being perpendicular to the strike of the trough strongly suggests that this extension is driven by the rotation of the segment instead of being related to some general process of back arc expansion.

[27] The Erromango-Futuna Trough ends near 20°S and is prolonged southward by a NE-SW transverse arc structure and by the NNW-SSE Aneytum Trough that terminates at 20.75°S where active volcanism occurs (Gemini Seamounts, GS in Figure 10). Seismicity indicates that the *T* axis slightly turns in this area compared to the Erromango-Futuna Trough, as do Ω_S small circles. The direction of extension is ENE-WSW, orthogonal to the trend of the Aneytum Trough, unlike the Futuna Trough. Because these elements are alternatively almost parallel and orthogonal to Ω_S small circles, it is proposed that they mark the southern extent of arc kinematics corresponding to Ω_S. The fact that clockwise rotation of this segment stops at around 21°S suggests incipient collision between the LR and the NH trench between 21° and 22°S.

3.6. North Vanuatu: Rapid Convergence, Counterclockwise Rotation, and Extension in the Northern Troughs

[28] At 13°S, the site in the Torres Islands (TORS) is the northernmost site observed in the present study. The observed rate of convergence relative to the Australian plate at TORS is 65 ± 5 mm/yr oriented N254° ± 3°. Motion relative to the WNFB is 25 ± 5 mm/yr oriented N101° ± 8°. At 14°S, the Banks Islands are active volcanic edifices associated with subduction along the arc. Accordingly, they lie about 100 km east of the trench. The GPS site is set on Mota Island (MOTA), an abandoned edifice on the eastern side of the Banks Islands. This site lies directly south of the junction between the HHR and the NH platform. Observed convergence rate relative to the Australian plate is 76 mm/yr oriented N266°. Motion relative to the WNFB is 15 mm/yr oriented N050°. According to these results, convergence at the NH trench is higher in north Vanuatu than in Central Vanuatu although it remains lower than A/P by 15–20 mm/yr.

[29] The pole Ω_N poorly predicts motions at TORS and MOTA. Indeed, the E-W component of the predicted motions are opposite in sign to those observed. It is worth noting that the velocity derived by GPS at TORS might be biased by some strain accumulation. Indeed, the Torres Islands have a very peculiar position, abnormally close to the trench (Figure 11). *Taylor et al.* [1985] showed that these islands undergo long-term uplift, suggesting that shallow, strong plate coupling occurs in this area. Such a strong coupling has been recently highlighted by the M_s 7.9 Torres thrust-type earthquake that occurred in January 1997. No GPS data from Torres Island were available prior to the quake. Simulations of interseismic elastic deformation using

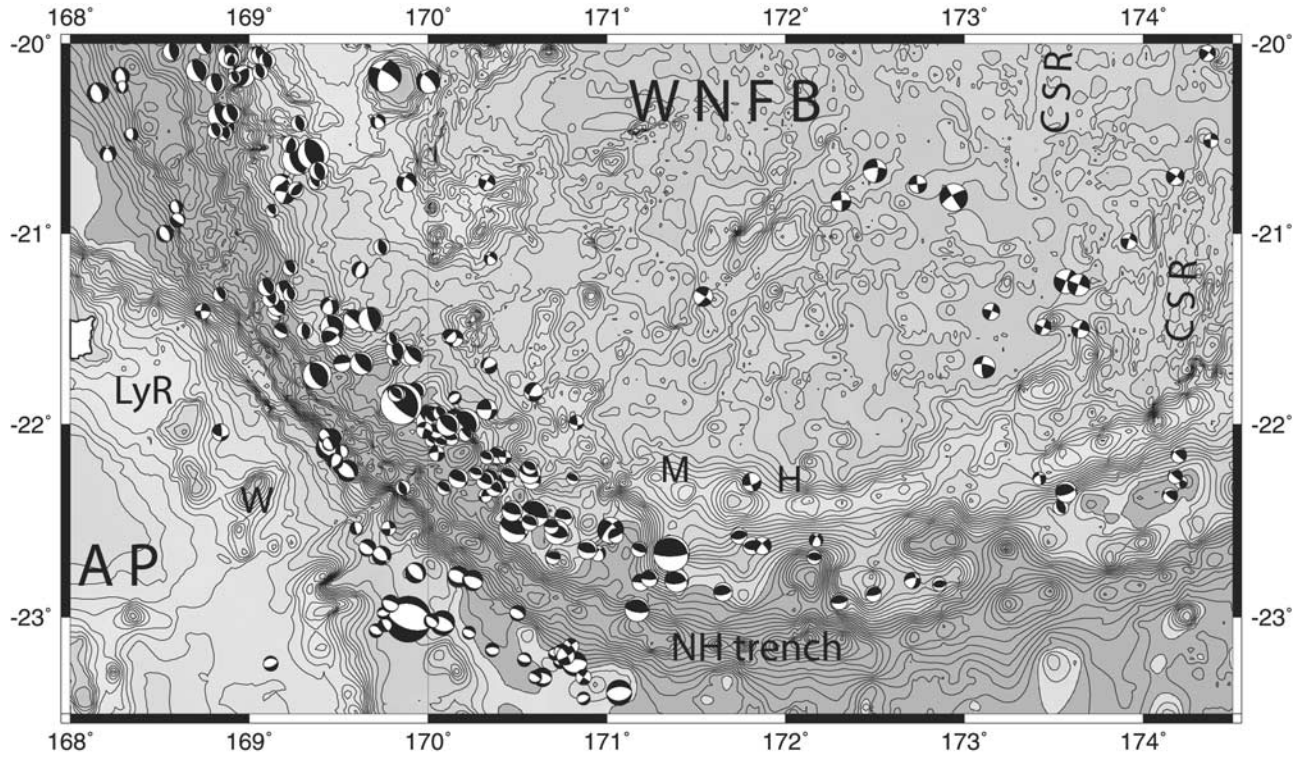

Figure 12. Bathymetric map of the southern termination of the New Hebrides subduction zone. Contour interval is 200 m. Focal mechanism solutions are shown for shallow earthquakes (<50 km, Centroid Moment Tensor Solutions, location NEIC) for the period 1977–2002 (size of circles as function of magnitude of event, lower hemisphere projection). Labels: AP, Australian plate; WNFB, western North Fiji Basin; NH trench, New Hebrides trench; W, Walpole Islet; M, Matthew Island; H, Hunter Island; and CSR, Central Spreading Ridge. See color version of this figure in the HTML.

a dislocation model [*Okada*, 1985], the focal parameters published by *Kaverina et al.* [1998], and assuming that the loading velocity at the locked plate interface is the convergence velocity, suggest that loading at TORS could be as large as 20 mm/yr, trending eastward. Thus the E-W long-term component of convergence at TORS could be higher by almost 20 mm/yr than the velocity derived from the existing GPS time series. In such a case, the motion of TORS relative to the WNFB would be negligible, in better agreement with the pole-derived motion. Also, no more back arc compression is required, indicating that the BATB should vanish around the latitude of the Torres Islands. This is in good agreement with the end of the back arc seismic lineament at 13.4°S characterized by thrust-type focal mechanism solutions (Figure 7).

[30] In another respect, it can be tested whether Ω_N might describe the rotation of the northern overriding NH platform, from Central Vanuatu to the eastern Solomon Islands. *Pelletier et al.* [1998] reported that extension in the northern back arc troughs (NBAT in Figure 11) at the latitude of the northern end of the NH trench, could be as high as 80 mm/yr, trending nearly eastward. The extension rate in the NBAT, at 166.5°E–10.5°S, i.e., at the northern edge of the platform, simulated using Ω_N is 81 ± 2 mm/yr oriented N265° ± 5°, which agrees very well with inferences by *Pelletier et al.* [1998]. Note that such a direction of extension is supported by major E-W trending fault scarps east of Reef and Santa Cruz Islands (Figure 11). Accordingly, pole-derived convergence relative to the Australian plate is 161 ± 2 mm/yr oriented N255° ± 5° at the northern virgation of the NH trench, in agreement with the 150–170 mm/yr predicted by *Pelletier et al.* [1998]. At 167.3°E, 12.8°S, two normal fault-type events northeast of the Torres Islands show evidence for extension in the trough (Figure 11), the *T* axis of which trends N127° and N132°. There Ω_N-derived motion is also extensional, trending N102° ± 6° at 36 ± 1 mm/yr. However, focal mechanisms in the region of 166.5°–167°E, 10.5°–11°S correspond to WSW-ENE extension.

[31] Therefore although the location of the Ω_N pole is not well constrained, in particular because observed motions in the Torres and Banks archipelagoes are not consistent with a pole south of 13°S, the northward increase in convergence velocity along the northern segment of the NH platform predicted by *Pelletier et al.* [1998] is well restituted by the anticlockwise rotation of Ω_N derived in this study. The lack of direct measurements in the eastern Solomon Islands currently prohibits any better modeling of the motions in this area. Subsequently, the connections between the northern and central segments, i.e., the northern termination of the BATB, cannot be concluded by this study.

3.7. Southern Termination of the NH Trench: Partitioning of Convergent Motion Into Trench-Parallel and Trench-Normal Components

[32] The GPS-derived convergence vectors established at the southern termination of the NH trench are derived with large uncertainties due to a combination of short observa-

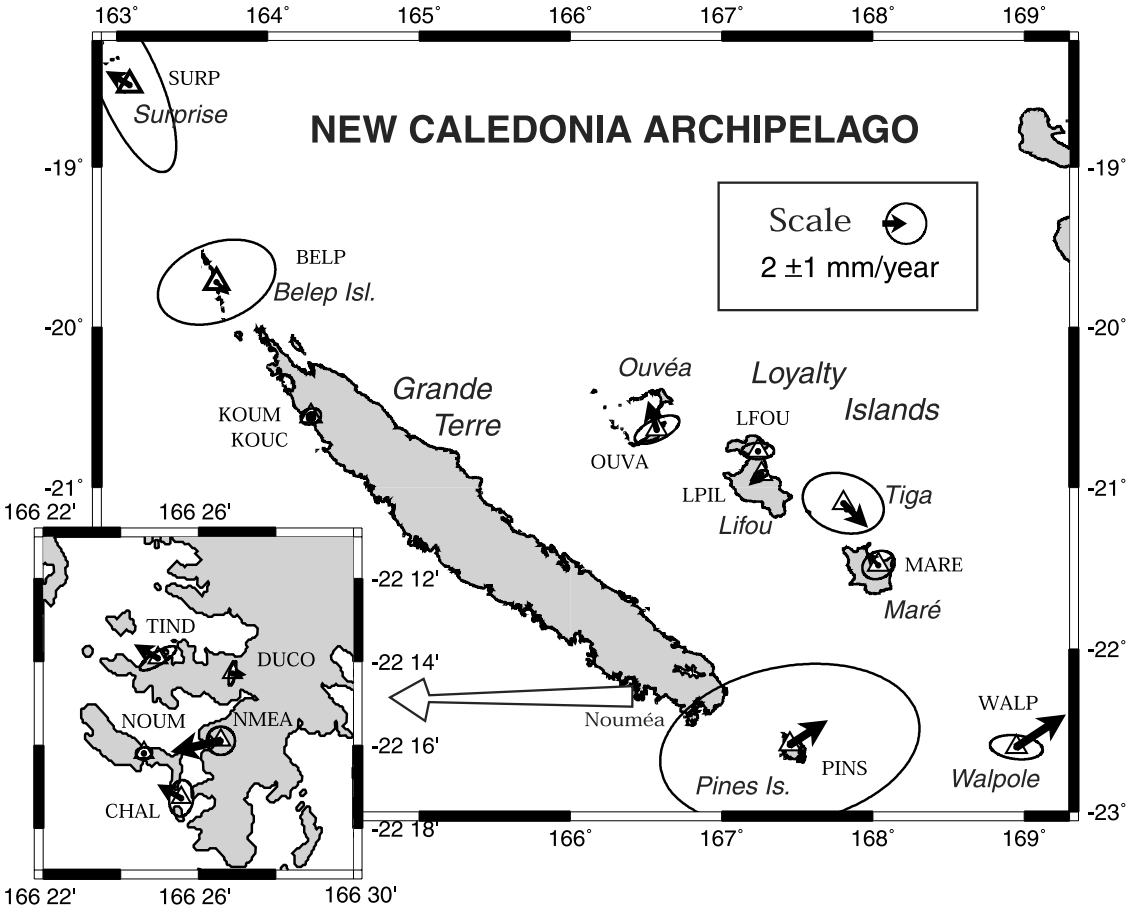

Figure 13. Residual velocities in the New Caledonia archipelago after local best adjustment.

Table 6. Motions of Sites of the New Caledonia Network With Respect to the Pole of the Australian Plate Determined in this Study (Ω_A)[a]

Island	Site Location	Name	Hor. Velocity wrt Ω_A	Number of Campaigns	Time Window
			Grande Terre (*Norfolk Ridge*)		
Koumac	**164.29°E 20.56°S**	**KOUC**	**0.0 ± 0.3 N000° ± 180°**	**CGPS**	**1996–2001**
Koumac	164.29°E 20.56°S	KOUM	0.6 ± 0.5 N271° ± 39°	9	1992–2001
Nouméa	**166.41°E, 22.27°S**	**NOUM**	**0.0 ± 0.4 N000° ± 180°**	**CGPS**	**1998–2001**
Nouméa	**166.44°E, 22.26°S**	**NMEA**	**4.2 ± 0.7 N257° ± 10°**	**CGPS**	**1997–1998**
Nouméa	166.41°E, 22.27°S	TIND	2.6 ± 0.6 N292° ± 8°	9	1990–1999
Nouméa	166.41°E, 22.27°S	DUCO	0.7 ± 0.4 N151° ± 18°	17	1993–2001
Nouméa	166.41°E, 22.27°S	CHAL	2.9 ± 0.7 N298° ± 16°	12	1992–2001
			Loyalty Islands		
Lifou	**167.26°E, 20.92°S**	**LPIL**	**1.3 ± 0.3 N229° ± 11°**	**CGPS**	**1996–2001**
Lifou	167.26°E, 20.92°S	LFOU	0.9 ± 0.7 N236° ± 36°	19	1990–2001
Ouvéa	166.57°E, 20.64°S	OUVA	2.2 ± 0.5 N336° ± 22°	5	1992–1998
Maré	168.04°E, 21.48°S	MARE	1.8 ± 0.7 N313° ± 21°	14	1990–2000
Tiga	167.80°E, 21.10°S	TIGA	3.0 ± 1.8 N153° ± 40°	2	1998–2000
Walpole	168.95°E, 22.60°S	WALP	5.0 ± 1.1 N057° ± 10°	11	1992–1995/1995–2000
			Other New Caledonia Islands on the Norfolk Ridge		
Surprise	163.09°E, 18.48°S	SURP	2.9 ± 3.9 N301° ± 91°	2	1993–1994
Belep	163.66°E, 19.72°S	BELP	0.7 ± 2.0 N137° ± 178°	2	1998–2000
Isle of Pine	167.45°E, 22.59°S	PINS	3.1 ± 6.2 N056° ± 100°	3	1998–2000

[a]A "/" indicates that the time series was interrupted by a coseismic step that year.

Table 7. Motions of Sites of the New Caledonia Network With Respect to Euler Pole Ω_{NC}[a]

Island	Site Location	Name	Residual Velocity wrt Ω_{NC}, mm/yr	
			Horizontal Component	Vertical Component
		Grande Terre (*Norfolk Ridge*)		
Koumac	**164.29°E, 20.56°S**	**KOUC**	**0.0 ± 0.3 N000° ± 180°**	**0.0 ± 0.5**
Koumac	164.29°E, 20.56°S	KOUM	0.0 ± 0.6 N271° ± 39°	0.0 ± 1.0
Nouméa	**166.41°E, 22.27°S**	**NOUM**	**0.0 ± 0.5 N000° ± 180°**	**0.0 ± 0.6**
Nouméa	**166.41°E, 22.27°S**	**NMEA**	**4.2 ± 0.7 N257° ± 10°**	**0.3 ± 2.2**
Nouméa	166.41°E, 22.27°S	TIND	2.2 ± 0.5 N300° ± 8°	**0.1 ± 1.5**
Nouméa	166.41°E, 22.27°S	DUCO	1.2 ± 0.2 N151° ± 18°	**−0.2 ± 0.7**
Nouméa	166.41°E, 22.27°S	CHAL	2.2 ± 0.7 N300° ± 21°	**0.1 ± 4.2**
		Loyalty Islands		
Lifou	**167.26°E, 20.92°S**	**LPIL**	**1.3 ± 0.3 N229° ± 11°**	**0.6 ± 0.6**
Lifou	167.26°E, 20.92°S	LFOU	0.0 ± 0.9 N000° ± 180°	**0.0 ± 2.0**
Ouvéa	166.57°E, 20.64°S	OUVA	2.4 ± 0.6 N342° ± 22°	**0.4 ± 1.6**
Maré	168.04°E, 21.48°S	MARE	1.4 ± 0.7 N316° ± 27°	**−0.2 ± 0.7**
Tiga	167.80°E, 21.10°S	TIGA	2.8 ± 2.0 N136° ± 41°	**0.3 ± 7.3**
Walpole	168.95°E, 22.60°S	WALP	5.0 ± 1.1 N057° ± 10°	**−6.4 ± 5.6**
		Other New Caledonia Islands on the Norfolk Ridge		
Surprise	163.09°E, 18.48°S	SURP	2.2 ± 3.9 N301° ± 119°	**0.2 ± 7.7**
Belep	163.66°E, 19.72°S	BELP	1.4 ± 2.0 N137° ± 86°	**0.1 ± 5.8**
Isle of Pine	167.45°E, 22.59°S	PINS	3.7 ± 6.3 N058° ± 83°	**0.2 ± 7.7**

[a] Ω_{NC} in rd/yr: $X = 6.477 \pm 7.066 \times 10^{-10}$, $Y = -1.830 \pm 1.764 \times 10^{-10}$; $Z = 2.036 \pm 2.836 \times 10^{-10}$.

tions, the use of poorly calibrated Leica GPS antennas, and the occurrence of the Walpole earthquake in May 1995. Relatively to the Australian plate, they notably differ both in modulus and orientation from A/P vectors (Figure 4) that predict mostly strike-slip motion along this portion of the trench, which runs almost parallel to the A/P relative motion. *Louat and Pelletier* [1989] inferred from the seismicity occurring in this area that some residual N-S convergence might occur between the North and South Fiji Basins. The change in azimuth in the slip vectors, which turn along the strike of the trench and remain normal to the trench, was also invoked in that study to propose that no strike-slip motion is accommodated at the plate boundary and that some kind of transform fault within the overriding plate should accommodate the differential motion between the Tanna and Matthew blocks. The convergence rates reported here (∼45 mm/yr, Table 3) indicate that convergence between the North and South Fiji Basins is in fact ongoing. Indeed, the GPS convergence vector is even larger than the projection of the A/P vector in this direction. This platelet is not being accreted to the Australian plate.

[33] Observed motions of Matthew (MTTW) and Hunter (HUNT) relative to the WNFB are, respectively, 87 mm/yr trending N108° and 101 mm/yr trending N102°. These values correspond to the largest motions relative to the NFB reported in the present study for islands belonging to the NH arc. They imply that a major E-W trending strike-slip boundary runs north of these islets, the existence of which has already been inferred by *Louat and Pelletier* [1989] and *Pelletier et al.* [1998], although it could not be recognized in the bathymetry lacking dense measurements in this area.

[34] Our data set includes a CGPS in the Fiji Islands (SUVA, Figure 3). The motion of this site relative to the Australian plate (1.1 ± 2.4 mm/yr oriented N304°) is negligible and not significant. Thus the Fiji platform appears motionless with respect to the Australian plate, as hypothesized by *Dubois et al.* [1977] and *Louat and Pelletier* [1989], and indicated by *Bevis et al.* [1995]. This suggests that the Conway-Kandavu lineament (CKL in Figure 1) that continues the Matthew-Hunter zone on the northeast is an inactive structure. The eastward motion of Matthew and Hunter Islets relative to the WNFB is consistent with a total rate of opening of 90–100 mm/yr at the northwest termination of the Fiji platform (Figure 1) [*Pelletier et al.*, 1998]. Conversely, it is significantly greater than the spreading rate reported at the southern termination of the Central Spreading Ridge (CSR) [50–60 mm/yr, *Huchon et al.*, 1994; 80 mm/yr, *Auzende et al.*, 1995]. Our data therefore suggest that the geometry and kinematics of spreading centers in the southernmost part of the NFB is likely not fully understood.

[35] At 22°S, the LR, born by the Australian plate, interacts with the NH arc (Figure 12). It has long been proposed that this interaction is responsible for the change in convergence in this area [*Louat and Pelletier*, 1989; *Pelletier et al.*, 1998], based on the change in seismicity observed at the trench virgation and tectonic evidence that the overriding margin at the zone of interaction was actually affected by the collision [*Monzier et al.*, 1984, 1990; *Maillet et al.*, 1989]. However, *Fitch* [1972] and *McCaffrey* [1992] showed that large obliquity in plate relative motion favors slip partitioning and development of strike-slip faulting within the overriding plate. In this case, obliquity increases eastward and is almost perpendicular at the southern termination of the NH trench. Interaction of a ridge born by the subducting plate and the overridding plate can strongly affect the trench-normal component of the convergence vectors, as evidenced in this paper by the Central Vanuatu case, but this does not occur at Matthew and Hunter. The vectors relative to the Australian plate at Matthew and Hunter are normal to the trench, trending, respectively, N197° and N177°. Relative to the WNFB, they trend southeastward, respectively, N108° and N102° (Table 3), that is nearly alongstrike the trench. Vectors thus trend perpendicular to each other when reported relative to the

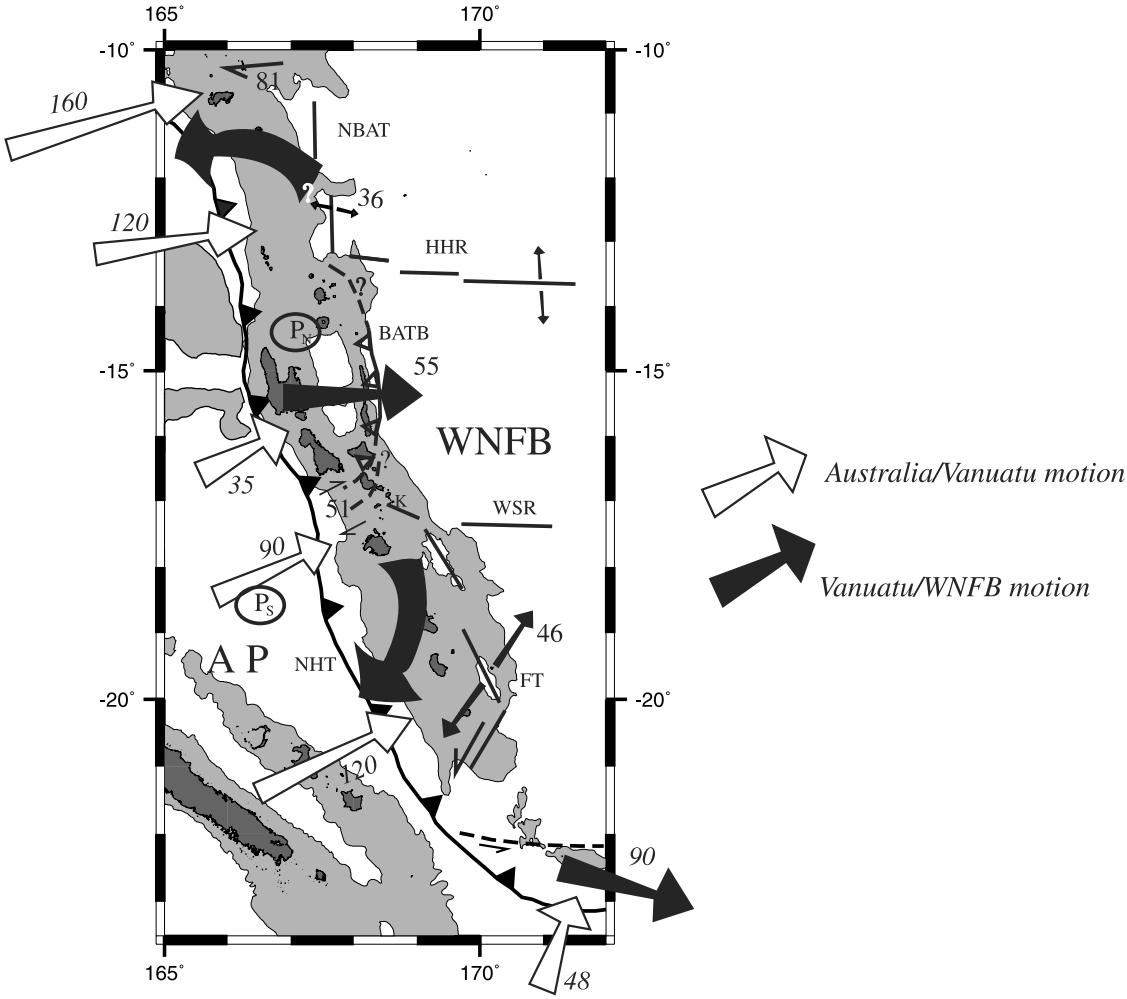

Figure 14. Tectonic setting of the New Hebrides arc derived from this study. Black arrows indicate motion relative to the WNFB. White arrows indicate convergence relative to the Australian Plate. Motions are in millimeters per year. Labels: AP, Australian Plate; WNFB, western North Fiji Basin; NHT, New Hebrides Trench; BATB, Back Arc Thrust Belt; NBAT, Northern Back Arc Trough; HHR, Hazel Holme Ridge; WSR, Western Spreading Ridge; FT, Futuna Trough; K, Kuwae volcano; P_S, pole of Ω_S; and P_N, pole of Ω_N.

overriding or to the subducting plate. It is therefore possible that the motion of the Matthew-Hunter block in fact reflects partitioning of the relative motion between the Australian and WNFB plates into trench-normal and trench-parallel components. However, large uncertainties affect the GPS-derived vectors and this part of the basin is almost devoid of in situ data away from the collision area. Whether the shear zone in the overriding plate implied by the motion of the Matthew-Hunter block reflects slip partitioning or was induced by interaction with the LR cannot be resolved. The corollary is that whatever the origin of the shear at the back of the block, the motion of that block, isolated between the fault and the trench, roughly conforms with the rules of slip partitioning.

3.8. New Caledonia and Loyalty Islands: Stability of the Eastern Australian Plate

[36] Sixteen sites were observed within this archipelago, including Grande Terre and other remote islands of the Norfolk Ridge, and all of the Loyalty Islands, including Walpole Islet (Figure 13). Residual motions of these sites relative to the Australian plate are reported in Table 6. RMS discrepancy between observed velocities for NC sites and velocities predicted by Ω_A is 1.2 mm/yr. The unit covariance factor is 0.85, supporting that uncertainties are realistic. This archipelago is thus globally motionless with respect to an Australian plate modeled by Ω_A.

[37] In order to check for any possible deformation within the network spread over the NC archipelago, we removed the geographically correlated part of these residuals by removing the Euler pole best fitting these residuals. This pole, named Ω_{NC}, is reported in Table 7. There is no statistically significant motion of the NC archipelago relative to Ω_A since the modulus of Ω_{NC} is comparable to its uncertainties and since it primarily reduces apparent vertical motions, which we have not accounted for when fitting rotations to a rigid plate assumption. The resulting velocity residuals are reported in Table 7.

[38] Recent works have reported that some active deformation might take place in NC [*Regnier et al.*, 1999] or on

the LR [*Lafoy et al.*, 1996]. Holocene extensional tectonics is evidenced in the south of Grande Terre (Y. Lagabrielle et al., manuscript in preparation) and in the Southern Lagoon [*Cabioch et al.*, 1996; *Lafoy et al.*, 2000]. The absence of relative motion between NOUM and KOUC, situated at opposite ends of this island, indicates that there is likely no deformation presently occurring within Grande Terre. Conversely, the remote sites of SURP and PINS, located on the Norfolk ridge, respectively, in northern and southern ends of the Grande Terre Island, present larger residuals. Given that the velocities for these sites were determined from just a few observations (two to three sessions) spanning a period of only 2–3 years, we conclude that more data have to be collected at these sites before such residuals can be regarded as evidence for deformation or segmentation of the Norfolk Ridge. These observations can, however, establish an upper bound of ~2 mm/yr for rates of potential horizontal deformation within the Norfolk ridge that bears the Grande Terre Island of NC. Also, it is worth noting that no significant deformation is recorded within the LR, or between the Loyalty and Norfolk ridges.

[39] Site WALP is set on Walpole Islet at a latitude of 22.6°S (Figure 12), south of the area where the LR and Vanuatu platforms interact. The large residual velocity derived for this site (Table 7) may indicate either left-lateral strike slip motion within the LR or strain accumulation. In May 1995, Walpole Islet experienced the largest (M_w = 7.7) normal-type earthquake ever recorded in such a context of elastic bulging prior to subduction [*Calmant et al.*, 2000]. The related coseismic step derived from the GPS time series is small and imprecise, 9 ± 7 mm oriented N116° ± 24°, much too small to produce the 5 mm/yr deformation rate observed. Besides, seismicity shows no evidence of active strike-slip faulting within the LR and this hypothesis is also unlikely. Mismodeling of the series due to either poor quality of the data collected or to site instability (the coral capping the islet is crosscut by large cracks) is also a likely explanation for this large velocity residual.

[40] Recently, *Beavan et al.* [2002] and *Sella et al.* [2002] found opposed results regarding the rigidity of the Australia place in the vicinity of the NH trench. The absence of noticeable deformation within the whole NC archipelago or relative to the rest of the Australia plate found in the present study supports Beavan's results.

4. Conclusion

[41] The GPS data collected over a decade in Vanuatu and NC give precise crustal motions all along the NH arc and sheds new light on the tectonics of this area. Large variations of convergence relative to the Australian plate are observed along the strike of the NH subduction zone. In Central Vanuatu, more convergence is accommodated at the rear than at the front of the arc, suggesting an ongoing reversal of the active converging boundary between the Australian plate and NFB in this area. The NH arc appears split into four segments, in close relationship to the subduction of aseismic ridges. The motion of the arc from 10 to 21°S, i.e., excluding the southernmost segment, is successfully modeled by a pair of Euler poles with opposite rotations (Figure 14). Both rotations combine in Central Vanuatu to produce an eastward translation of this area. The two blocks on either side of the central block rotate in opposite ways. Rotation of the lateral segments result in a combination of partial coupling at the boundary shared with the central segment and extension in the longitudinal back arc troughs, extension that increases away from the central segment. The southernmost segment is located south of the interaction of the NH arc with the LR. The motion at this segment is split into trench-normal and trench-parallel components. Whether this partitioning of motion is due to convergence obliquity or interaction of the margin with the LR is not resolved.

[42] The two cases of ridge subduction addressed in this study appear to produce markedly different tectonic schemes. In front of the DER, the overriding margin is bulldozed and the motion of lateral margin segments is likely also affected by the collision. In front of the much massive LR, no dramatic thrust structure is evidenced within the margin, and it is not clear whether the collision or the convergence obliquity is responsible for the lateral shift of the Matthew-Hunter block. Given that the LR just started interacting with the NH margin 0.5 Ma ago, whereas the DER subduction last since about 2 Ma, the latter may stand for a mature evolution of the former, incipient. A jump of the plate boundary in front of the collision area would stand for the end stage of the process.

[43] As far as the subducting plate is concerned, no significant horizontal deformation could be evidenced either between the NC archipelago and the rest of the Australian plate or within the archipelago itself, except the coseismic step recorded at Walpole Islet.

[44] **Acknowledgments.** The project was funded by the Institut de Recherche pour le Développement (IRD), the National Science Foundation (NSF), and the French "Programme National sur les Risques Naturels." This project has also benefited from the support of the New Caledonia and Vanuatu Survey Departments. Authors are indebted to the surveyors who performed the GPS observations in often severe and hazardous conditions, especially to J.-M. Bore, J.-L. Laurent, M. Kalsale Williams, and J.-C. Willy. Authors are also indebted to the French Navy authorities who provided the logistical support for the operations conducted on the Walpole, Matthew, and Hunter Islets. Authors thank T. Kato who provided the C-GPS data from the WING project in Western Pacific, P. Tregoning for fruitful discussions, and reviewers for helpful comments. UMR GeoAzur contribution 509.

References

Auzende, J. M., B. Pelletier, and J. P. Eissen, The North Fiji basin: Geology, structure and geodynamic evolution, in *Back-Arc Basin: Tectonics and Magmatism*, edited by B. Taylor, pp. 139–175, Plenum, New York, 1995.

Beavan, J., P. Tregoning, M. Bevis, T. Kato, and C. Meertens, Motion and rigidity of the Pacific Plate and implications for plate boundary deformation, *J. Geophys. Res.*, *107*(B10), 2261, doi:10.1029/2001JB000282, 2002.

Bevis, M., et al., Geodetic observations of very rapid convergence and back-arc extension at the Tonga arc, *Nature*, *374*, 249–251, 1995.

Cabioch, G., J. Recy, C. Jouannic, and L. Turpin, Contrôle climatique et tectonique de l'edification récifale en Nouvelle Calédonie au cours du Quaternaire terminal, *Bull. Soc. Geol. Fr.*, *167*, 729–742, 1996.

Calmant, S., P. Lebellegard, F. Taylor, M. Bevis, D. Maillard, J. Recy, and J. Bonneau, Geodetic measurements of convergence across the New Hebrides subduction zone, *Geophys. Res. Lett.*, *22*, 2573–2576, 1995.

Calmant, S., B. Pelletier, R. Pillet, M. Regnier, P. Lebellegard, D. Maillard, F. Taylor, M. Bevis, and J. Recy, Interseismic and coseismic motions in GPS series related to the M_s 7.3 July, 13, 1994, Malekula earthquake, Central New Hebrides Subduction Zone, *Geophys. Res. Lett.*, *24*, 3077–3080, 1997.

Calmant, S., J. J. Valette, J. F. Cretaux, and L. Soudarin, Tectonic plate motion and co-seismic steps surveyed by DORIS field beacons: The New-Hebrides experiment, *J. Geod.*, *74*, 512–518, 2000.

Collot, J. Y., J. Daniel, and R. Burne, Recent tectonics associated with the subduction/collision of the D'Entrecasteaux zone in the central New Hebrides, *Tectonophysics*, *112*, 325–356, 1985.

De Mets, C., R. Gordon, D. Argus, and S. Stein, Effects of recent revisions to the geomagnetic reversal time scale on estimates of current plate motions, *Geophys. Res. Lett.*, *21*, 2191–2194, 1994.

Dubois, J., J. Launay, J. Recy, and J. Marshall, New Hebrides trench: Subduction rate from associated lithospheric bulge, *Can. J. Earth Sci.*, *14*, 250–255, 1977.

Ebel, J., Source processes of the 1965 New Hebrides Islands earthquakes inferred from the teleseismic waveforms, *Geophys. J. R. Astron. Soc*, *63*, 381–403, 1980.

Eissen, J.-P., et al., Rapport de mission de la campagne CALVA, 12–18 Juillet 1996, 34 pp., 9 annexes, Centre de Brest, Brest, France, 1997.

Fitch, T., Plate convergence, transcurrent faults and internal deformation adjacent to southeast Asia and western Pacific, *J. Geophys. Res.*, *77*, 4432–4460, 1972.

Frohlish, C., M. F. Coffin, C. Massell, P. Mann, C. Schuur, S. D. Davis, T. Jones, and G. Karner, Constraints on Macquarie Ridge tectonics provided by Harvard focal mechanisms and teleseismic earthquake locations, *J. Geophys. Res.*, *102*, 5029–5041, 1997.

Huchon, P., E. Gracia, E. Ruellan, M. Joshima, and J.-M. Auzende, Kinematics of active spreading in the North Fiji Basin (southwest Pacific), *Mar. Geol.*, *116*, 69–87, 1994.

Isacks, B. L., R. Cardwell, J. L. Chatelain, M. Barazangi, J. M. Marthelot, D. Chinn, and R. Louat, Seismicity and tectonics of the central New Hebrides island arc, in *Earthquake Prediction: An International Review*, *Maurice Ewing Ser.*, vol. 4, edited by D. W. Simpson and P. G. Richards, pp. 93–116, AGU, Washington, D. C., 1981.

Kaverina, A., D. Dreger, and M. Antolik, Source process of the 21 April, 1997 Santa Cruz Island earthquake (M_w 7.8), *Geophys. Res. Lett.*, *25*, 4027–4030, 1998.

Lafoy, Y., F. Missegue, D. Cluzel, and R. Le Suave, The Loyalty-New Hebrides arc collision: Effects on the Loyalty ridge ad basin system, southwest Pacific (first results of the ZoNeCo Programme), *Mar. Geophys. Res.*, *18*, 337–356, 1996.

Lafoy, Y., J.-M. Auzende, R. Smith, and C. Labails, Evolution géologique post-Pléistocène moyen du domaine lagonaire Néo-Calédonien méridional, *C. R. Acad. Sci. Paris*, *330*, 265–272, 2000.

Lagabrielle, Y., et al., Active oceanic spreading in the northern North Fiji Basin. Results of the NOFI cruise of the *R/V L'Atalante*, *Mar. Geophys. Res.*, *18*, 225–247, 1996.

Larson, K., and J. Freymueller, Relative motions of the Australia, Pacific and Antarctic plates estimated by the Global Positioning System, *Geophys. Res. Lett.*, *22*, 37–40, 1995.

Larson, K., J. Freymueller, and S. Philipsen, Global plate velocities from the Global Positioning System, *J. Geophys. Res.*, *102*, 9961–9981, 1997.

Louat, R., and B. Pelletier, Seismotectonics and present-day relative plate motion in the New Hebrides arc-North Fiji basin region, *Tectonophysics*, *167*, 41–55, 1989.

Louat, R., M. Hamburger, and M. Monzier, Shallow and intermediate depth seismicity in the New Hebrides arc: Constraints on the subduction process, in *Geology and Offshore Ressources of Pacific Islands Arcs-Vanuatu Region*, *Earth Sci. Ser.*, vol. 8, edited by H. G. Green and F. L. Wong, pp. 279–286, Circum-Pac. Counc. for Energy and Miner. Res., Houston, Tex., 1988.

Maillet, P., M. Monzier, J. P. Eissen, and R. Louat, Geodynamics of an arc-ridge junction: The case of the New Hebrides Arc/North Fiji Basin, *Tectonophysics*, *165*, 251–268, 1989.

Maillet, P., E. Ruellan, M. Gerard, A. Person, H. Bellon, J. Cotten, J.-L. Joron, S. Nakada, and R. Price, Tectonics, magmatism, and evolution of the New Hebrides back-Arc troughs (southwest Pacific), in *Back-Arc Basins, Tectonics and Magmatism*, edited by B. Taylor, pp. 177–235, Plenum, New York, 1995.

McCaffrey, M., Oblique plate convergence, slip vectors, and forearc deformation, *J. Geophys. Res.*, *97*, 8905–8915, 1992.

Monzier, M., P. Maillet, J. Foyo Herrera, R. Louat, F. Missegue, and B. Pontoise, The termination of the southern New Hebrides subduction zone (southwestern Pacific), *Tectonophysics*, *101*, 177–184, 1984.

Monzier, M., J. Daniel, and P. Maillet, La collision "ride des Loyauté/arc des Nouvelles Hébrides" (Pacifique Sud-Ouest), *Oceanol. Acta*, *10*, 43–56, 1990.

Monzier, M., C. Robin, and J.-P. Eissen, Kuwae (~1425 A.D.): The forgotten caldera, *J. Volcanol. Geotherm. Res.*, *59*, 207–218, 1994.

Okada, Y., Surface displacement due to shear and tensile faults in a half-space, *Bull. Seismol. Soc. Am.*, *75*(4), 1135–1154, 1985.

Pelletier, B., P. Charvis, J. Daniel, Y. Hello, F. Jamet, R. Louat, P. Nanau, and P. Rigolot, Structure et linéations magnétiques dans le coin nord-ouest du bassin Nord-Fidjien: résultats préliminaires ed la campagne EVA14 (aout 1987), *C. R. Acad. Sci. Paris*, *306*, 1247–1254, 1988.

Pelletier, B., M. Meschede, T. Chabernaud, P. Roperch, and X. Zhao, Tectonics of the central New Hebrides arc, North Aoba basin, *Proc. Ocean Drill. Program Sci.*, *Results,134*, 431–444, 1994.

Pelletier, B., S. Calmant, and R. Pillet, Current tectonics of the Tonga-Nw Hebrides region, *Earth Planet. Sci. Lett.*, *164*, 263–276, 1998.

Pelletier, B., et al., Le séisme d'Ambrym-Pentecote (Vanuatu) du 26 Novembre 1999 (M_w: 7.5): Données préliminaires sur la séismicité, le tsunami et les déplacements associés, *C. R. Acad. Sci. Paris*, *331*, 21–28, 2000.

Price, R. C., and L. Kroenke, Tectonics and magma genesis in the northern North Fiji basin, *Mar. Geol.*, *98*, 241–258, 1991.

Recy, J., et al., Tectonique et volcanisme sous-marin à l'arrière de l'arc des Nouvelles Hébrides (Vanuatu, Pacifique Sud-Ouest): résultats préliminaires de la campagne SEAPSO Leg II du N/O Jean Charcot, *C. R. Acad. Sci. Paris*, *303*, 685–689, 1986.

Recy, J., B. Pelletier, P. Charvis, M. Gerard, M. C. Monjaret, and P. Maillet, Structure, âge et origine des fossés arrière-arc des Nouvelles Hebrides (Sud Ouest Pacifique), *Oceanol. Acta*, *10*, 165–182, 1990.

Regnier, M., S. Van de Beuque, C. Baldassari, and G. Tribot Laspiere, La sismicité du Sud de la Nouvelle-Calédonie: Implications structurales, *C. R. Acad. Sci. Paris*, *329*, 143–148, 1999.

Regnier, M., S. Calmant, B. Pelletier, Y. Lagabrielle, and G. Cabioch, The Mw 7.5 1999 Ambrym earthquake, Vanuatu: A back arc intraplate thrust event, *Tectonics*, *22*, doi:10.1029/2002TC001422, in press, 2003.

Rotacher, M., G. Beutler, W. Gurtner, E. Brockman, and L. Nervart, Documentation for Bernese GPS Software Version 3.4, Univ. of Bern, Bern, Switzerland, 1993.

Schutz, R., M. Bevis, F. Taylor, D. Kuang, M. Watkins, J. Recy, B. Perrin, and O. Peyroux, The southwest Pacific GPS project: Geodetic results from burst 1 of the 1990 field campaign, *Bull. Geod.*, *67*, 234–240, 1993.

Sella, G. F., T. H. Dixon, and A. Mao, REVEL: A model for Recent plate velocities from space geodesy, *J. Geophys. Res.*, *107*(B4), 2081, doi:10.1029/2000JB000033, 2002.

Sillard, P., Z. Altamini, and C. Boucher, The ITRF96 realization and its associated velocity field, *Geophys. Res. Lett.*, *25*, 3223–3226, 1998.

Smith, D. E., Kolenkiewicz, R. S. Nerem, P. J. Dunn, M. H. Torrence, J. W. Robbins, S. M. Klosko, R. G. Williamson, and E. C. Pavlis, Contemporary global horizontal crustal motion, *Geophys. J. Int.*, *119*, 511–520, 1994.

Taylor, F. W., B. Isacks, C. Jouannic, A. Bloom, and L. Dubois, Coseismic and quaternary vertical tectonic movements, Santo and Malekula islands, New Hebrides island arc, *J. Geophys. Res.*, *85*, 5367–5381, 1980.

Taylor, F. W., C. Jouannic, and A. Bloom, Quaternary uplift of the Torres islands, northern New Hebrides frontal arc: Comparison with Santo and Malekula islands, Central New Hebrides frontal arc, *J. Geol.*, *93*, 419–438, 1985.

Taylor, F. W., C. Frolich, J. Lecolle, and M. Strecker, Analysis of partially emerged corals and reef terraces in the central Vanuatu arc: Comparison of contemporary coseismic and nonseismic with quaternary vertical movements, *J. Geophys. Res.*, *92*, 4905–4933, 1987.

Taylor, F. W., R. Edwards, G. Wasserburg, and C. Frohlich, Seismic recurrence intervals and timing of aseismic subduction inferred from emerged corals and refs of the central Vanuatu (New Hebrides) frontal arc, *J. Geophys. Res.*, *95*, 393–408, 1990.

Taylor, F. W., M. Bevis, B. Schutz, D. Kuang, J. Recy, S. Calmant, D. Charley, M. Regnier, B. Perin, M. Jackson, and C. Reichenfeld, Geodetic measurements of convergence at the New Hebrides island arc indicate arc fragmentation caused by an impinging aseismic ridge, *Geology*, *23*, 1011–1014, 1995.

Tregoning, P., Plate kinematics in the western Pacific derived from geodetic observations, *J. Geophys. Res.*, *107*(B1), 2020, doi:10.1029/2001JB000406, 2002.

Tregoning, P., et al., Estimation of current plate motions in Papua New Guinea from Global Positioning System observations, *J. Geophys. Res.*, *103*, 12,181–12,203, 1998.

M. Bevis and D. A. Phillips, Hawaii Institute for Geophysics and Planetology, School of Ocean and Earth Science and Technology, University of Hawaii, Honolulu, HI 96822, USA.

S. Calmant, Laboratoire de Géophysique et Océanographie Spatiale, IRD, 18 Av E. Belin, Toulouse F-31500, France. (calmant@notos.cst.cnes.fr)

P. Lebellegard and B. Pelletier, Laboratoire de Géophysique, Centre IRD, BP A5, Nouméa, New Caledonia.

F. W. Taylor, Institute for Geophysics, University of Texas at Austin, 4412 Spicewood Springs Rd., Building 600, Austin, TX 78759-8500, USA.